Adaptation of human cell populations to different levels of centriole amplification involves a two-step response

Marco António Dias Louro[1,2,3,#,*], Catarina Peneda[1,4,#,**], Claudia Bank[2,3], Mónica Bettencourt-Dias[1,***]

[1.] Instituto Gulbenkian de Ciência, Oeiras, Portugal

[2.] Institut für Ökologie und Evolution, Universität Bern, Bern, Switzerland

[3.] Swiss Institute of Bioinformatics, Lausanne, Switzerland

[4.] Instituto de Ciências Biomédicas Abel Salazar, Universidade do Porto, Porto, Portugal

[#] These authors contributed equally to this work

*Correspondence: mlouro@igc.gulbenkian.pt

**Correspondence: catarinasapeneda@gmail.com

***Correspondence: mdias@igc.gulbenkian.pt

Summary

Centrioles are the main components of cilia and centrosomes, which play a central role in cell proliferation and signalling. Their number is strictly regulated. Centriole amplification, or the presence of extra centrioles, often occurs in tumours and leads to aneuploidy and altered signalling and has been associated with cancer development and malignancy. Negative selection of cells with extra centrioles prevents numerical errors from expanding in the population, resulting in an overproduction-selection balance. However, how chronic perturbation of key centriolar regulators affect centriole number dynamics is poorly described.

PLK4, a key regulator of centriole biogenesis, is often overexpressed in cancer and is associated with worse prognosis in breast cancer. Here we show that centriole amplification cannot be sustained in cultured MCF10A breast cells exposed to low and high levels of chronic PLK4 overexpression. We observed a short-term response in which negative selection and reduction in PLK4 mRNA limit centriole amplification. This was followed by long-term adaptation in which a rise in PLK4 mRNA levels was decoupled from accumulation of the protein at the centrosome. Furthermore, adaptation was dose-dependent. Populations evolved in low-overexpression conditions retained the ability to generate extra centrioles when PLK4 was further overexpressed, whereas centriole overproduction was irreversibly inhibited in populations evolved under high PLK4 overexpression. Taken together, our data reveal a two step mode of centriole number regulation and suggest that differences in the level of PLK4 overexpression may condition cancer evolution.

Introduction

The centrosome, found in most animal cells, plays a key role in organising microtubules, cell polarity, signalling, and proliferation. The canonical centrosome consists of two centrioles and a surrounding pericentriolar matrix that nucleates microtubules. During the cell cycle, each centriole duplicates once, so that in mitosis, each pair of centrioles migrates to opposite poles of the cell and directs the organisation of a bipolar mitotic spindle[1–5]. Abnormal centriole numbers can induce several changes in cell physiology. During mitosis they can cause mitotic defects that lead to chromosome segregation errors and aneuploidy and can affect cell cycle progression and viability[6–10]. In interphase, they are associated with altered secretion and signalling which can promote invasiveness[11–13]. Centriole amplification is known to be widespread in human tumours and has been associated with poor prognosis in several types of cancer, including breast cancer[14–17]. Moreover, centriole amplification is already present in pre-malignant conditions suggesting a possible role in early cancer development[18]. Furthermore, centriole amplification was shown to promote tumour initiation in mouse models[19,20]. Understanding the causes of centriole amplification and how cells respond to this perturbation is therefore vital for exploring its role in cancer development.

Centriole number is highly controlled in most cells. Even cancer-derived cell lines, which show different baseline levels of centriole amplification[21], usually display a characteristic distribution of centriole numbers per cell. When these levels are transiently altered, centriole numbers usually revert to their original distribution[10,22–25]. This suggests that the processes that lead to an increase or decrease in the number of centrioles eventually balance each other out, producing a stable equilibrium[26].

Centriole amplification can occur through various mechanisms, such as changes in the concentration or activity of centriolar components[27–31], or due to failure in cytokinesis[32]. Cells with too many centrioles might divide abnormally and/or undergo cell cycle arrest, leading to reduced proliferation or even cell death. Thus, centriole numbers appear to be maintained at an equilibrium by a balance of centriole overproduction and negative selection acting on cells with extra centrioles[26,33]. However, most studies are limited to investigating short-term effects and transient centriole number alterations. The long-term dynamics of centriole numbers, especially in cancer where centriole-related proteins are often overexpressed[34,35], remain poorly understood. Thus, understanding these dynamics in scenarios of chronic perturbation is crucial for a comprehensive view of centrosome regulation.

PLK4, an essential centriole biogenesis regulator, plays a significant role in centriole number dynamics. Several studies showed that overexpressing PLK4 leads to centriole amplification, whereas reducing its expression can prevent centriole duplication[27,28]. In cultured cells, short-term chronic PLK4 overexpression leads to proliferation defects that limit the proliferation of cells bearing extra centrioles[6,36]. In mice, it was proposed that mild PLK4 overexpression is associated with persistent centriole amplification and cancer development[19,20]. In contrast, it was suggested that cells with high levels of expression are negatively selected[36–38]. However, this hypothesis has not been tested. Although PLK4 overexpression is common in cancers like breast cancer and acute myeloid leukaemia[39–41], where centriole amplification has been observed, the impact of these gene expression changes on centriole number dynamics is not known. This study aims to explore how different PLK4 overexpression levels affect centriole number dynamics and cell population fitness over time.

We used MCF10A cells carrying a doxycycline-inducible system to trigger PLK4 overexpression[11] at different levels. Over two months we monitored centriole numbers, conducted competition assays for fitness and proliferation, and tracked PLK4 levels. We found that cell populations overexpressing PLK4 eventually returned to normal centriole numbers. However, whereas populations evolved under high PLK4 overexpression, irreversibly lost their ability to form more centrioles in response to doxycycline, this was not the case for low PLK4 overexpression, which could still respond to higher concentrations, suggesting different evolutionary trajectories. Moreover, while PLK4 mRNA levels decreased initially, they later matched or exceeded those in the initial population. Our results support a model in which cells respond to PLK4 overexpression in a two-step regulatory process: a short-term phase with negative selection and transcriptional regulation limiting the proliferation of cells with extra centrioles, and a long-term phase in which high PLK4 levels are prevented from accumulating at the centrosome.

Results

An experimental framework for addressing the evolution of cell populations experiencing different levels of centriole amplification

In this study, we established an experimental framework for addressing the long-term overproduction-selection dynamics of populations with centriole amplification. We made use of overexpression of PLK4, as the trigger for centriole amplification. We chose to use MCF10A-PLK4, a cell line derived from non-transformed breast tissue[11], where PLK4 overexpression is induced by adding doxycycline (Dox) to the culture medium. This system is widely used to study the implications of altered centrosome number in cell physiology and breast cancer[11,13,21,42,43], widening the implications of our study.

We first sought to obtain cell populations with different initial degrees of centriole amplification. Tetracycline/doxycycline-inducible systems are known to display a sigmoidal dose response - i.e. the expression of target gene(s) rises sharply for intermediate levels of induction lead and plateaus when higher doses are applied[44]. This behaviour led us to search for optimal intermediate doses, which would lead to different levels of centriole amplification. Previously, we had observed that 24h treatment with doxycycline concentrations between 0.1 µg/mL and the typically used 2 µg/mL, yielded similar levels of centriole amplification (data not shown). Thus, we investigated the effect of treating MCF10A-PLK4 populations with concentrations of Dox ranging between 0 and 0.1 µg/mL for 24h (Fig. 1A, B). Since centriole numbers change along the cell cycle, we analysed mitotic cells, which are expected to have four centrioles, allowing us to estimate the degree of centriole number abnormalities more accurately. We observed a significant and dose-dependent increase in the relative frequency of mitotic cells with extra centrioles in Dox-treated populations compared to the control without Dox. Treatment with 0.001 µg/mL of Dox resulted in approximately 29% of cells with extra centrioles. Between 0.005 and 0.1 µg/mL of Dox, the relative frequency of mitotic cells with extra centrioles plateaued at around 60-70% (Fig. 1B). Given that we observed significant differences in the level of centriole amplification in populations treated with Dox at 0, 0.001, and 0.1 μg/mL, we selected these concentrations for further investigation. We will refer to them hereafter as Dox0, Dox0.001 and Dox0.1.

To assess the consequences of long-term chronic PLK4 overexpression and centriole amplification, we designed an experimental evolution setup (Fig. 1C). Experimental evolution aims at characterising how evolutionary forces, such as natural selection or genetic drift, shape populations because of the established test conditions[45]. We were interested in testing if and how cell populations subject to chronic PLK4 overexpression adapt to centriole amplification and how this might occur. MCF10A-Plk4 is a polyclonal cell line, thus containing genetic and phenotypic variation that may allow cells to cope with PLK4 overexpression or centriole amplification. Second, we evolved cells for two months (approximately 90 generations according to published doubling times for regular MCF10A in control conditions), which is sufficient for selection to act while preventing excessive accumulation of mutations. Third, we passaged cells every three days at a high seeding density ($2.2x10^6$ cells) and allowed them to reach a large population size (~$2x10^7$ cells in control conditions). This setup provided us control over the population growth dynamics and enabled us to minimise genetic drift.

Given that both Dox alone[46] and PLK4 catalytic activity[47] may induce physiological effects beyond centrosome amplification we added different controls to our experiment. We controlled for other consequences of expressing PLK4 and adding Dox using two different cell lines: 1) MCF10A-PLK4$^{1-608}$, which carries a Dox-inducible truncated form of PLK4, which includes the kinase domain but not its C-terminus necessary to locate it to the centriole. Thus, its overexpression does not result in centriole overproduction[11,48] and 2) MCF10A-TetR, the parental cell line of MCF10A-PLK4 and MCF10A-PLK4$^{1-608}$, which carries the Dox-inducible system but not a target transgene. Thus, our setup included three different cell lines in three different cell culture media (containing 0, 0.001, or 0.1 µg/mL of Dox), which we evolved for two months (Fig. 1C).

This setup allowed us to assess a variety of cellular parameters over time. We sampled MCF10A-TetR, MCF10A-PLK4$^{1-608}$, and MCF10A-PLK4 populations grown with 0, 0.001, or 0.1 *µ*g/mL of Dox at days 1, 3, 16, 31, 46, and 64 for centriole number counting and RNA extraction. In addition, we performed competition assays in the beginning (starting at day 1), middle (starting at day 31) and at the end of the experiment (starting at day 64). This enabled us to estimate population fitness over time, as well as to assess cell proliferation, cell death, and cell cycle profiles using flow cytometry. Finally, we monitored population growth using automated cell counting during passaging.

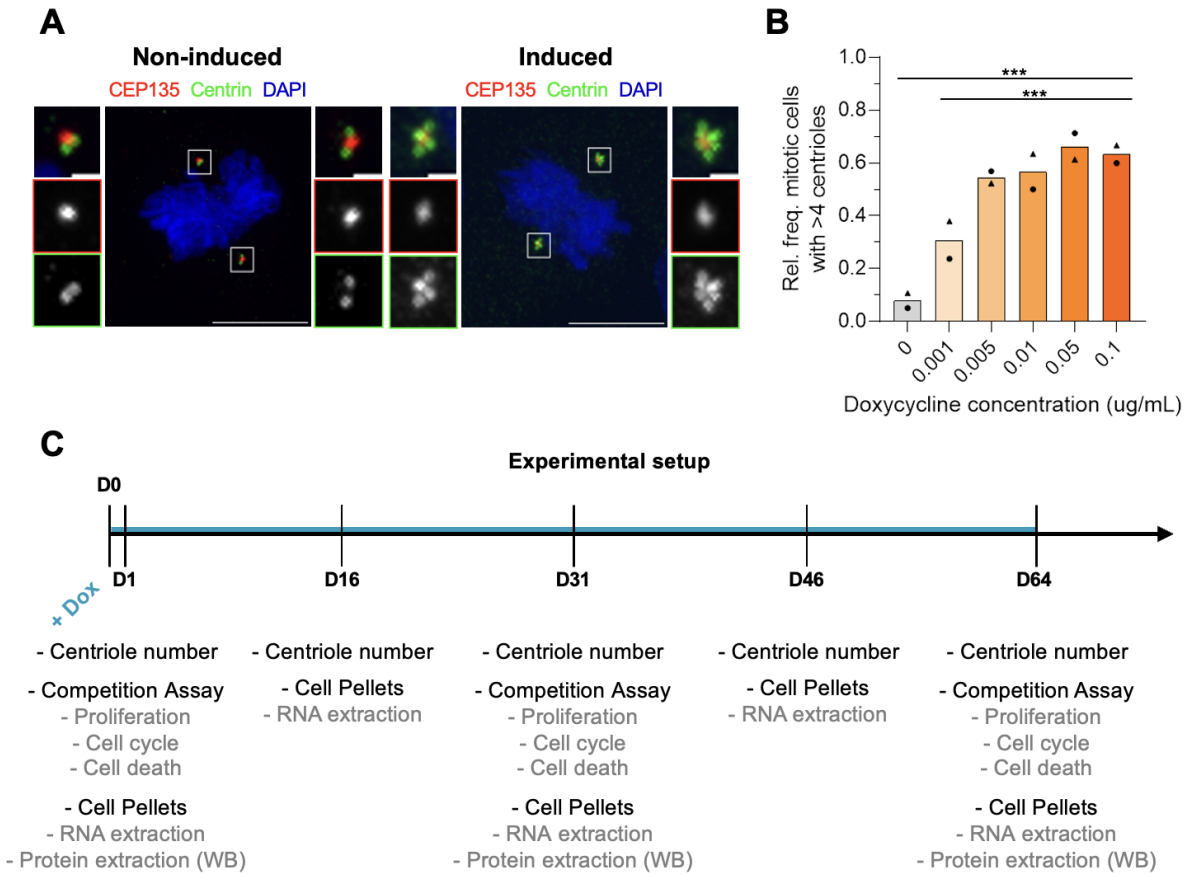

Figure 1. Experimental framework for addressing the evolution of cell populations experiencing different levels of centriole amplification. **A -** Example of mitotic cells with wild-type (left) and abnormally high (right) centriole numbers. Cells were stained for CEP135 (magenta), Centrin (green),

and DNA (blue). Scale bar is 10 nm. **B -** Relative frequency of mitotic cells with more than four centrioles following 24h treatment with the indicated doses of doxycycline. Symbols represent different replicates. 62-100 mitotic cells were analysed in each of the two independent experiments. **C-** Experimental evolution setup and conditions. MCF10A-TetR, MCF10A-PLK4$^{1-608}$ and MCF10A-PLK4 populations were grown for two months in media containing doxycycline at 0, 0.001, or 0.1 µg/mL and sampled for centriole number counting, competition assays, and pellets for RNA extraction and western blots, at the indicated time points.

Centriole number dynamics depend on the initial centriole amplification levels in MCF10A-PLK4

We first asked how centriole numbers change in cell populations chronically treated with different doses of doxycycline. As expected, the relative frequency of cells with extra centrioles showed no significant differences over time in the negative controls MCF10A-TetR and MCF10A-Plk4$^{1-608}$, regardless of Dox (Fig. 2A-B, Fig. S1), and in non-induced MCF10A-PLK4 (Fig. 2C). In contrast, the relative frequency of mitotic cells with centriole amplification in Dox0.001- and Dox0.1-treated MCF10A-PLK4 reached an average of 28±4% and 91.5±5.5% after 24h, respectively, compared with 7±2% for the non-induced population, and steadily decreased in subsequent days (Fig. 2C). The number of centrioles per mitotic cell was highest, on average, and most variable at day 1 (mean centriole number: Dox 0 - 4.18±0.02, Dox0.001 - 5.24±0.26 , Dox0.1 - 12,84±2.14; Fig. 2D-F). Over time, both the mean and variance of centriole numbers per cell reverted to basal levels for both Dox concentrations (Fig. 2D-E). Finally, centriole amplification decreased more rapidly at higher Dox concentrations (Dox0 - 0.00173, *p*-value=0.97653, Dox0.001 - -0.23567, *p*-value=0.00128, Dox0.1 - -0.864769, *p*-value<2e^{-16}). This suggests that different PLK4 overexpression levels/incidence of cells with extra centrioles can elicit different selective pressures. We concluded that both low and high chronic Plk4 overexpression ultimately result in loss of centriole amplification, but with different dynamics. These results suggest that populations under chronic induction of PLK4 overexpression adapted by inhibiting overproduction or that continuous negative selection eliminated cells with extra centrioles, leading to a reduction in population fitness. Therefore, we investigated the fitness of these populations.

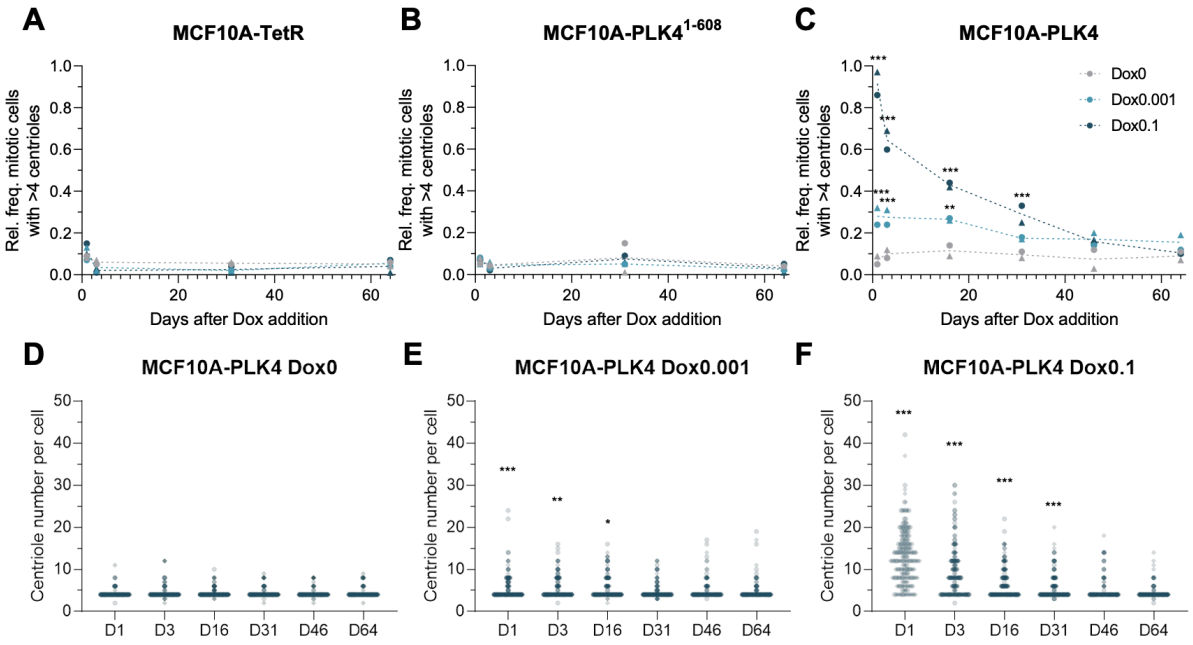

Figure 2: Centriole number dynamics depend on the initial centriole amplification levels in MCF10A-PLK4. A-C - Relative frequency of mitotic cells with more than four centrioles at the indicated time points of Dox treatment for MCF10A-TetR (A), MCF10A-PLK4$^{1-608}$ (B), and MCF10A-PLK4 (C). Data points correspond to populations grown in the presence of doxycycline at 0 (light grey), 0.001 (light blue), or 0.1 μg/mL (dark blue), dashed lines represent the average relative frequency of cells with more than four centrioles at each time point for populations grown in Dox0 (grey), Dox0.001 (light blue), or Dox0.1 (dark blue) and different shapes represent independent experiments. Statistical analysis were performed using a generalised linear model with the presence/absence of extra centrioles in a cell as a binomial response variable and taking Dox concentration and time point as independent categorical predictors, plus their interaction. Significant differences between the indicated condition and the one treated with Dox0 at the same time point are represented with ** (p-value < 0.01) or *** (p-value < 0.001). **D-F** - Centriole number distributions in MCF10A-PLK4 populations growth in Dox0 (D), Dox0.001 (E), and Dox0.1 (F). 72-100 mitotic cells were analysed for each condition in each of the two independent experiments.

MCF10A-PLK4 populations adapted to centriole amplification in a dose-dependent manner

Estimating competitive fitness requires a setup that allows populations to be distinguished in co-culture. To accomplish this, we labelled these populations with proliferation dyes, CellTrace CFSE and CellTrace Far Red[49].

To monitor population fitness over time, we performed competition assays in which we co-cultured MCF10A-PLK4 or the control MCF10A-PLK4$^{1-608}$ with the parental cell line, MCF10A-TetR. Each co-cultured population was labelled with a different proliferation dye and grown for three days (Fig. 3A). This time window allows for a clear separation of both sub-populations by flow cytometry and encompasses sufficient cell divisions for detecting fitness differences (Fig. S2). As technical controls, we performed replicate co-cultures stained with the opposite

combination of dyes, controlling for the effect of the dye on proliferation. Finally, we calculated the competitive index for each co-culture, a standard measure of competitive fitness[50] (see Methods).

Importantly, for all data points, we observed a good correlation between replicates and between different proliferation dye combinations (Fig. S2). Additionally, we observed no effect of the initial frequency of each co-cultured sub-population on competitive index estimates (Fig. S2). Together these suggest that the calculated index reflects changes in fitness and not experimental artefacts. As expected, control line MCF10A-PLK4$^{1-608}$ showed no significant fitness differences between different Dox concentrations when co-cultured with MCF10A-TetR at any time point (Fig. 3B Left panel). This is coherent with previous reports, in which short term overexpression of truncated PLK4 did not affect population growth[11]. However, we observed that Dox treatment imparted a significant and dose-dependent fitness cost in MCF10A-PLK4 relative to MCF10A-TetR at days 1-3 (Fig. 3B right panel). At days 31-33, the fitness cost associated with both Dox concentrations was highly reduced and we found it to be undetectable at days 64-66 (Fig. 3B right panel). These results suggest that the fitness cost observed in the induced MCF10A-PLK4 populations depends on the overexpression of full-length PLK4 and/or the presence of centriole amplification.

Our results led us to ask if the evolved populations, i.e. from the end point of the experiment, had adapted to the presence of Dox. Adaptation can be defined as a relative increase in fitness of the evolved populations compared with the ancestral populations, in the conditions in which they evolved[51]. To address this, we co-cultured the evolved MCF10A-PLK4 populations with the ancestral population in media with different Dox concentrations. Moreover, to ask whether Dox concentration led to differently adapted populations, we co-cultured each pair of evolved populations in different combinations of media (Fig. 3C).

As controls, we co-cultured each evolved and ancestral populations with themselves, and observed no significant fitness differences (Fig. 3C). The population evolved in Dox0.001 did not show significant fitness differences compared with the ancestral population in any media, indicating no significant adaptation in this condition (Fig. 3C). On the other hand, the population evolved in Dox0.1 outcompeted all the others at this concentration, suggesting it had adapted (Fig.3C).

Adaptation to an environment often involves molecular changes that can have a fitness cost if cells return to the ancestral environment[52]. Interestingly, when we co-cultured each of the three evolved populations with the ancestral population, or the population evolved without Dox, in media without Dox, we observed no significant fitness differences (Fig. 3C). These results suggest a negligible fitness cost of Dox adaptation.

In summary, (1) MCF10A-Plk4 populations adapted to high (Dox0.1) but not low levels (Dox0.001) of chronically-induced PLK4 overexpression; (2) there was no cost of adaptation; (3) exposing the populations evolved in Dox0 and Dox0.001 to higher doses of Dox still bears a fitness cost. Therefore, since adaptation to centriole amplification/PLK4 overexpression was dose-dependent, we hypothesised that populations grown in different doses of Dox may have developed distinct mechanisms that allow them to cope with PLK4 overexpression/centriole amplification (e.g. regulating PLK4 expression, or even completely silencing transgene, as

previously observed[37]). Notwithstanding, these putative mechanisms both resulted in the decrease of extra centrioles from the population.

Since our competition results suggest that the fitness depends on the level of centriole amplification, we asked if this could also explain the observed fitness differences between evolved populations. To address this, we quantified centriole numbers in each of the evolved populations treated with Dox0, 0.001, and 0.1 for 24h. Moreover, we tested if they could produce extra centrioles when treated with higher concentrations of Dox (2 µg/mg). As controls, we treated ancestral populations with the same range of Dox concentrations.

We observed that the ancestral MCF10A-PLK4 populations showed a proportional increase in the relative frequency of mitotic cells with extra centrioles when treated with 0.001 and 0.1 µg/mL of Dox for 24h (Fig. 4A, B), as observed above. Treatment with 2 µg/mL of Dox yielded no significant differences compared with 0.1 µg/mL. The populations that evolved in Dox0 showed an identical trend compared with the ancestral population but reached lower levels of amplification for each respective treatment. Populations evolved in Dox 0.001 did not show a response when grown in that medium or without Dox. However, they showed an increase in the relative frequency of cells with extra centrioles when exposed to 0.1 and 2 µg/mL of Dox. Concerning the population that evolved in Dox 0.1, none of the tested treatments yielded a significant increase in the relative frequency of mitotic cells with extra centrioles (Fig. 4A, B). This suggests that the mechanism of inhibition of centriole overproduction may be specific to the level of PLK4 overexpression.

Together with the previous competition assays, these results indicate that fitness differences between co-cultured populations could be explained by the level of centriole amplification. Indeed, we observed a significant correlation between the relative frequency of mitotic cells with extra centrioles and average competitive index (Fig 4C). We also observed a significant correlation between mean centriole number and average competitive index, albeit slightly weaker (Fig 4D). These results show that the level of centriole amplification, in particular, the relative frequency of cells with extra centrioles, can explain most of the observed variation in the competitive index.

In summary, our results suggest that evolution of cells in Dox0.1 leads to a loss of the ability to amplify centrioles in response to the tested concentrations of Dox. This is not observed in the population evolved in Dox0.001, where cells do not amplify centrioles in low Dox but maintain that ability in higher Dox concentrations. These results suggest the existence of different regulatory mechanisms or the same mechanism operating at different magnitudes, that counteract centriole amplification at low Dox and high Dox.

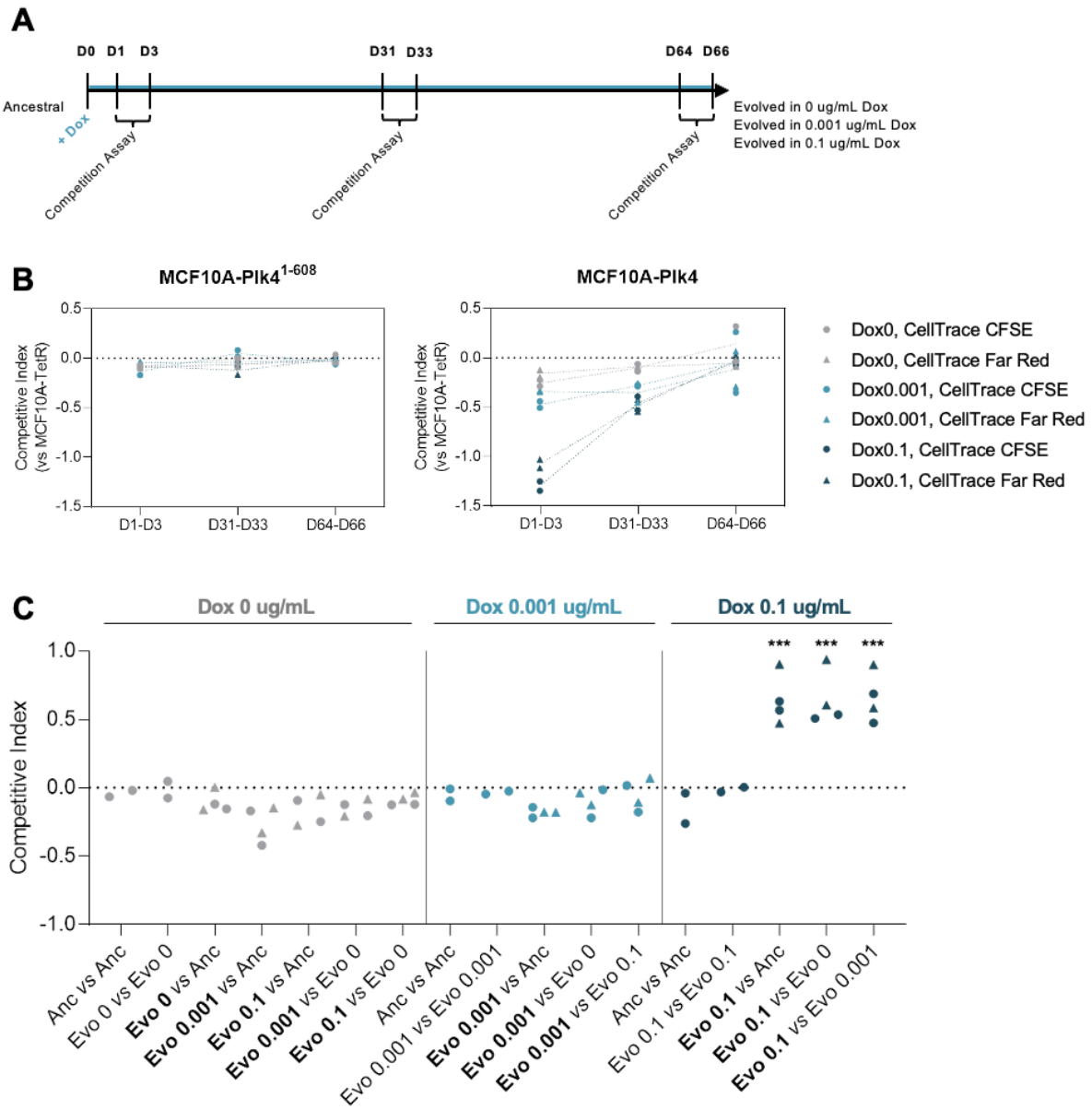

Figure 3. Induced MCF10A-PLK4 adapted over time to chronic PLK4 overexpression. A - Timeline for competition assays. Cells were labelled with different fluorescent dyes (CellTrace CFSE or Far Red) and co-cultured at the indicated time points. The competitive index was used as a proxy for competitive fitness based on the relative frequencies of each co-cultured population at the initial and final time points (see Methods). **B -** Competitive index of MCF10A-PLK4$^{1-608}$ (B) or MCF10A-PLK4 (C) relative to MCF10A-TetR at the indicated time points. Note that for each experimental situation there are 4 data points (independent experiments and swapping of the dye). The dashed lines connect the average competitive index corresponding to each Dox concentration and dye combination in two independent experiments. See table S1 and S2 for statistical analyses. **C -** Competitive index of evolved and ancestral MCF10A-PLK4 populations competing in the indicated combinations. Cell populations were co-cultured in medium with Dox0, Dox0.001, or Dox0.1. The points in the plots correspond to the competitive index of the cell line in bold. Circles correspond to populations labelled with CellTrace CFSE and triangles to populations labelled with CellTrace Far Red. Note that when a given population was co-cultured with itself, one sub-population was labelled with CellTrace CFSE and the other with CellTrace Far Red, i.e. there is only one combination of dyes. Data were modelled using a linear model (ANOVA) taking experimental conditions as a grouping variable. Significant differences between the

indicated conditions and their controls (ancestral versus ancestral and evolved versus evolved) are represented with *** (*p*-value<0.001).

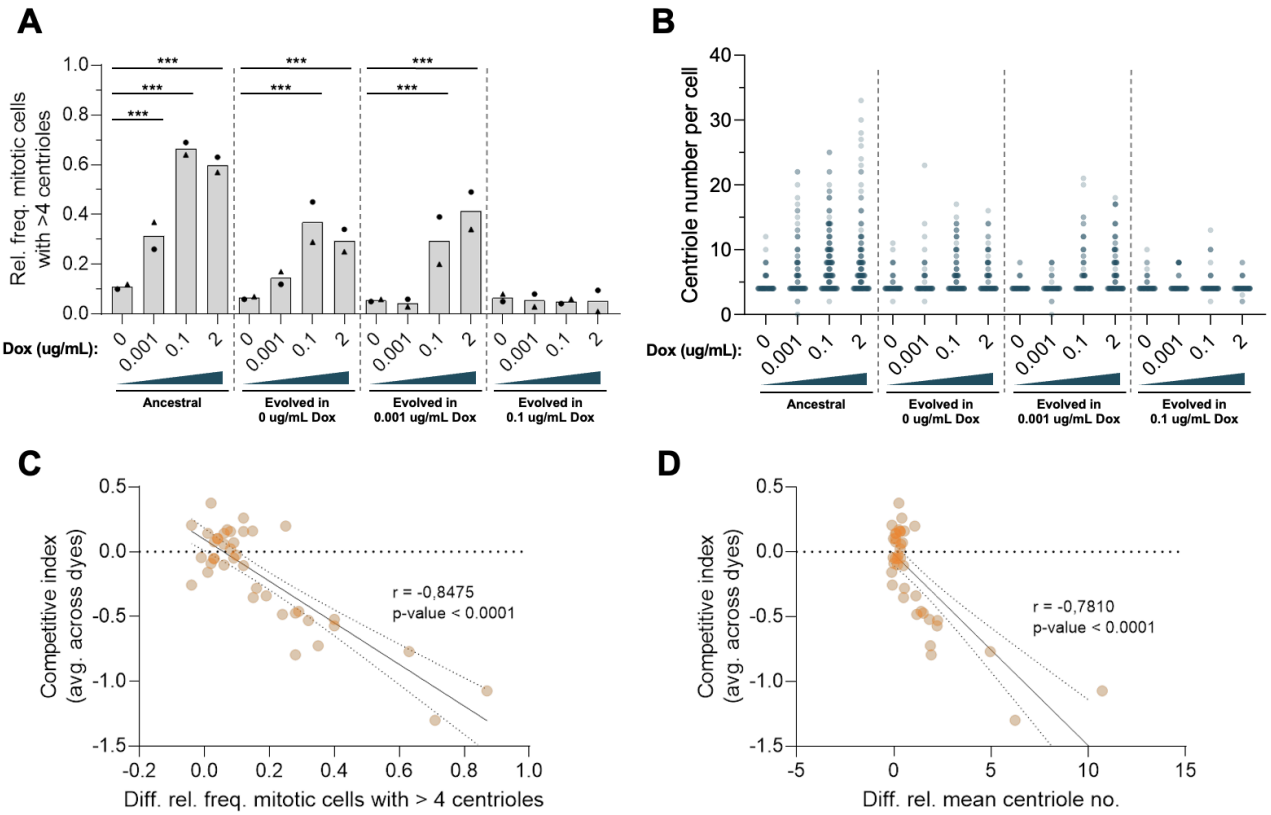

Figure 4. The fitness cost in ancestral and evolved populations is correlated with the level of centriole amplification. A - Relative frequency of mitotic cells with extra centrioles in ancestral and evolved MCF10A-PLK4 populations treated with Dox at the indicated concentrations for 24h. **B** - Centriole number distributions in ancestral and evolved MCF10A-PLK4 populations treated with Dox at the indicated concentrations for 24h. 95-100 cells were analysed for each condition in two independent experiments. Statistical analyses were performed using a generalised linear model with the presence/absence of extra centrioles in a cell as a binomial response variable and taking Dox concentration and population (ancestral, evolved in Dox0, evolved in Dox0.001, and evolved in Dox0.1) as independent categorical predictors, plus their interaction. Significant differences between the indicated condition and the one treated with Dox0 within the same population are represented with *** (*p*-value < 0.001). **C -** Correlation between average competitive index of the two dye combinations and the difference in the relative frequency of mitotic cells with more than four centrioles between co-cultured MCF10A-PLK4 and MCF10A-TetR. **D -** Correlation between average competitive index of the two dye combinations and the difference in mean centriole number in mitotic cells between co-cultured MCF10A-PLK4 and MCF10A-TetR. Data points include competitive indices calculated for three time points (at days 1-3, 31-33, and 64-66) and the corresponding centriole number data (at days 1, 31, and 64). The best fitting linear regression is indicated as a solid line. The dashed lines indicate the 95% confidence interval.

Slower proliferation explains the fitness cost of centriole amplification

Differences in competitive fitness can be due to changes in population growth. Centriole amplification can lead to defects in cell proliferation, cell cycle arrest and cell death[5,23]. Thus, we monitored the population size of the evolving populations by automated cell counting and calculated their relative growth rate compared with the Dox0-treated population. As expected, Dox treatment did not significantly affect the growth rate of control MC10A-TetR (Fig. S3A) and MCF10A-PLK4$^{1-608}$ (Fig. S3B), when compared with Dox0 over time. In addition, we observed no significant change in the growth of MCF10A-PLK4 grown in Dox 0.001, whereas in Dox 0.1, the relative growth rate of the population decreased up to day 8 and progressively returned to basal levels (Fig. S3C). These results suggest that fitness differences can be attributed to changes in population growth.

Population growth depends on the balance between cell proliferation and death. We first assessed cell death in our competition assay setup by flow cytometry using propidium iodide staining, which labels dead or dying cells. The relative frequency of viable cells was not affected by Dox treatment in any of the cell lines, at any time point (Fig. 5A-B) suggesting that the fitness cost in induced MCF10A-PLK4 populations cannot be explained by differences in cell death.

Secondly, we assessed cell proliferation by measuring the decay rates of CellTrace CFSE and CellTrace Far Red in our competition assay setup. After labelling, each daughter cell inherits, on average, half of the dye molecules present in the mother cell following mitosis. Thus, the rate of dye decay can be used as a proxy for the rate of cell division.

As a control, we found no effect of the proliferation dye or initial frequency of each population on relative dye decay rates. Moreover, the two replicates were well correlated, validating the methodology (Fig. S4). As expected, control MCF10A-PLK4$^{1-608}$ showed no significant differences in relative dye decay at any time point, regardless of Dox treatment (Fig. 5C). At days 1-3, the dye decay rate of induced MCF10A-PLK4 was significantly lower than MCF10A-TetR and was more affected by higher Dox concentration. This result suggests slower proliferation of cell populations with higher levels of centriole amplification (Fig. 5D). Importantly, over time, the relative dye decay rate of Dox0.001 and Dox0.1-treated MCF10A-PLK4 recovered at days 31-33, at which point only the population evolved in Dox0.1 showed significantly reduced decay rates. At days 64-66 (Fig. 5D) the relative dye decay rate of both Dox-treated populations was equal to MCF10A-TetR (relative dye decay close to 1). These results suggest that proliferation is the main factor impinging on fitness.

Several papers have now reported a potential non-cell-autonomous effect of centriole amplification. It was suggested that cells with centriole amplification secrete factors that promote invasion in neighbouring cells that do not show centriole amplification, thus contributing to changes in the microenvironment[9,23]. It is thus possible that cell proliferation is also sensitive to cell non-autonomous effects in the co-cultures. We tested this by performing mono-cultures and assessing for cell proliferation and comparing with the results in the co-cultures (Fig. 5E). We observed a good correlation between co-cultured and mono-cultured populations (Fig 5E), suggesting that potential non-cell-autonomous interactions between cells with and without centriole amplification did not affect their proliferative capacity.

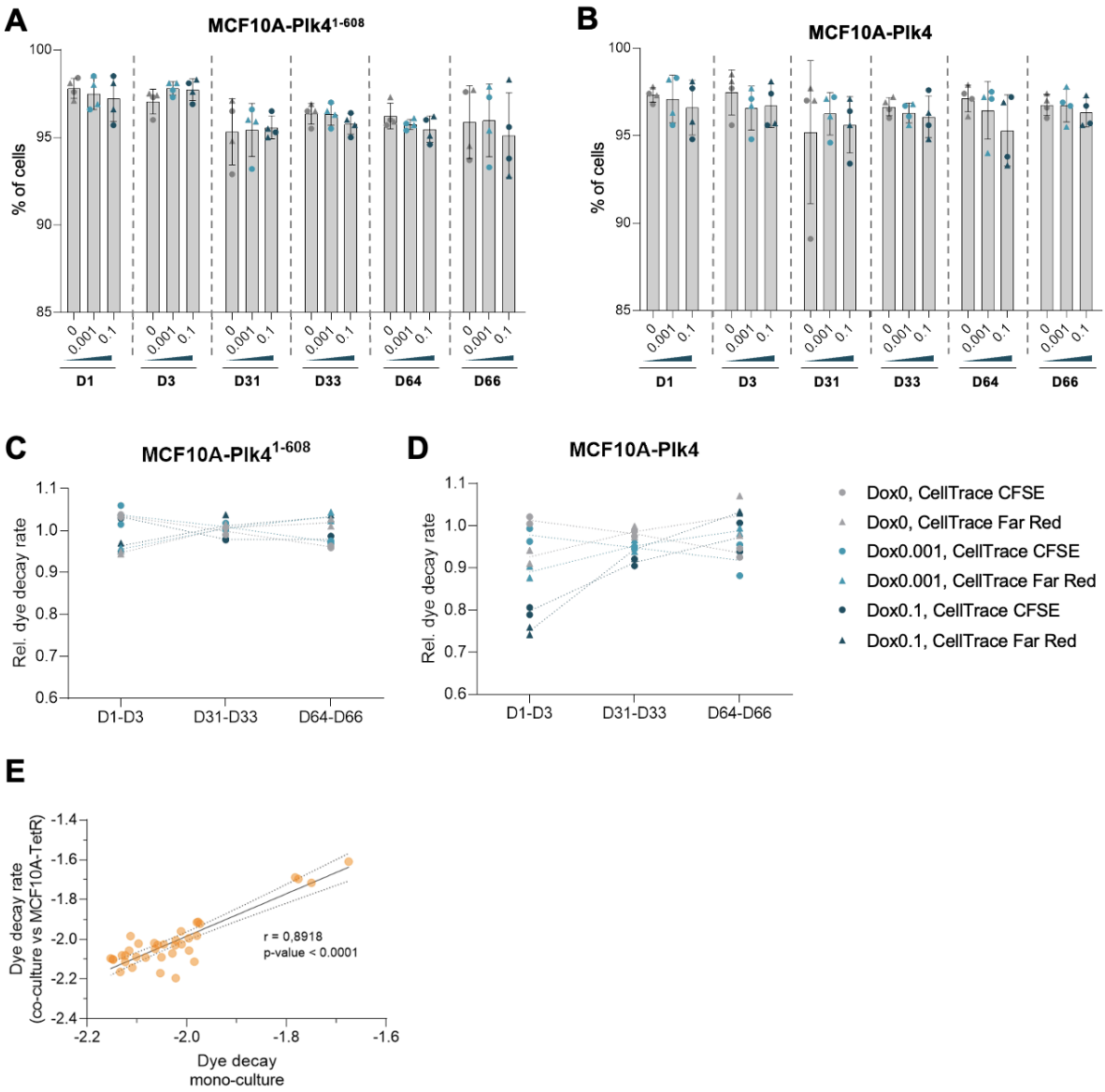

Figure 5: Slower proliferation explains the fitness cost of centriole amplification. A, B - Percentage of PI-negative MCF10A-PLK4$^{1-608}$ (A) or MCF10A-PLK4 (B) co-cultured with MCF10A-TetR at the indicated time points. Data corresponding to co-cultures are represented as circles (MCF10A-PLK4$^{1-608}$/MCF10A-PLK4 labelled with CellTrace CFSE) or triangles (MCF10A-PLK4$^{1-608}$/MCF10A-PLK4 labelled with CellTrace Far Red). **C, D -** Relative dye decay rate of MCF10A-PLK4$^{1-608}$ (C) or MCF10A-PLK4 (D) co-cultured with MCF10A-TetR at the indicated time points. The relative dye decay rate was calculated as a proxy for the rate of cell division. Data corresponding to co-cultures grown in Dox0 (light grey), Dox0.001 (blue), or Dox0.1 (dark blue) are represented as circles (MCF10A-PLK4$^{1-608}$/MCF10A-PLK4 labelled with CellTrace CFSE) or triangles (MCF10A-PLK4$^{1-608}$/MCF10A-PLK4 labelled with CellTrace Far Red). The dashed lines connect the average relative dye decay rate for each Dox concentration and dye combination in two independent experiments. See table S3 and S4 for statistical analyses. **E** - Correlation between dye decay rates of co-cultured (with MCF10A-TetR) and mono-cultured MCF10A-PLK4 populations at D1-3, D31-33, and D64-66. Data are represented as circles (MCF10A-PLK4 labelled with CellTrace CFSE) or triangles (MCF10A-PLK4 labelled with CellTrace Far Red). The best fitting linear regression is indicated as a solid line. The dashed lines indicate the 95% confidence interval.

The fitness cost of centriole amplification is correlated with G1 delay and p53 activation

Changes in proliferation resulting from centriole amplification were previously associated with cell cycle delays resulting from p53 activation[6,53–55]. We next tested whether the changes in fitness observed were associated with those alterations.

We analysed the cell cycle profiles, by staining cells with Hoechst 33342, in our competition assay setup. As expected, control MCF10A-TetR and MCF10A-PLK4$^{1-608}$ displayed no changes in their cell cycle profiles over time and for all Dox concentrations, either in mono-culture or in co-culture (Fig. 6A, Fig. S5). However, in MCF10A-PLK4 populations induced with Dox0.1 we observed that G1 cells were significantly overrepresented at day 3, both in mono-cultures and co-cultures (Fig. 6B, Fig. S5). Conversely, no significant differences were observed in the cell cycle profiles at days 31, 33 and 64, 66 consistent with the increase in fitness and dye decay rates observed at that time point, apart from a small reduction in the percentage of G1 cells at day 66 in the Dox0.1-treated population (Fig. 6B). No significant differences were observed in Dox0.001, in accordance with the reduced fitness costs observed for this condition. In summary, our data suggest that the initial fitness and proliferation deficit in Dox0.1 induced MCF10A-PLK4 populations results from a delay/arrest in G1.

We next assessed p53 activation in our setup in the MCF10A-PLK4 cell line at different time points and levels of Dox. Activation of p53 is usually associated with an increase in its abundance and nuclear translocation[56]. We analysed p53 levels by western blot (Fig. 6C, D) and p53 nuclear localisation by immunofluorescence as a proxy for its activation (Fig. 6E, F). Our western blot data showed an increase in p53 levels that was higher at high Dox concentration in the first three days of treatment compared to non-induced MCF10A-PLK4. Whereas this change was also observed at Dox0.001 it was faster in Dox0.1, starting on day 1 and was more pronounced in day 2 and 3 (Fig. 3C, D). At days 31 and 64, when we observed no effects in cell cycle (Fig. 6B) or proliferation (Fig. 5D), p53 levels in induced MCF10A-PLK4 at all Dox concentrations were similar to those of the non-induced population (Fig. 6C, D).

Consistently with total protein levels, we observed an increase in the relative frequency of interphase cells with nuclear p53 over the first three days of induction, which correlated positively with the concentration of Dox. At days 31 and 64, p53 nuclear localisation reverted to basal levels despite continuous Dox treatment (Fig. 6F). Thus, p53 was activated over the first three days of induction, correlating with the observed cell cycle arrest/delay and the strongest fitness cost, and its activation decreased as the populations adapted. Interestingly, the results show that both p53 activation and cell cycle changes recovered more rapidly than population fitness, which was still significantly reduced at D31-33, suggesting that other factors may have contributed to the observed fitness differences. In conclusion, we observed short term proliferation defects, p53 activation and cell cycle delay/arrest following chronic PLK4 overexpression, as previously observed[6,10], but these defects gradually disappeared over time, as the levels of centriole amplification decreased. This supports the idea that adaptation to long term induction of PLK4 overexpression occurred by suppression of centriole overproduction. We next tested potential molecular mechanisms associated with this adaptation.

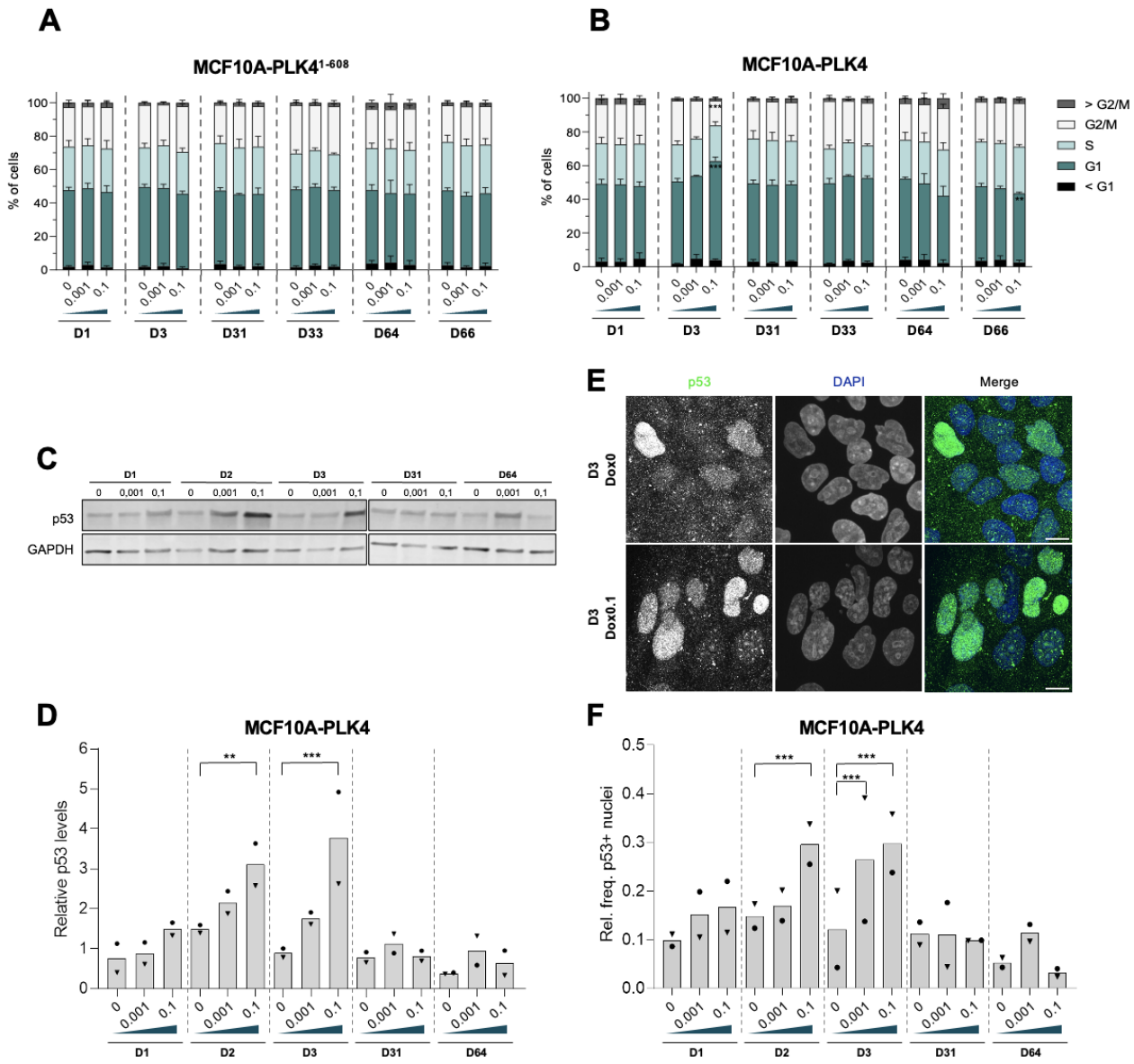

Figure 6: Cell populations with centriole amplification showed cell cycle defects and p53 activation. A, B - Relative frequency of cells in G1 (dark green), S (light green), and G2/M (white) for MCF10A-PLK4 (A) and MCF10A-PLK4 (B) in co-cultures at the indicated time points. Average relative frequencies of co-cultured populations in the respective cell cycle stage. The error bars represent the mean +- standard deviation. **C -** Representative immunoblot for p53 in MCF10A-PLK4 populations grown with the indicated Dox concentration, at the indicated time points. **D -** Quantification of p53 relative to GAPDH by immunoblotting in MCF10A-PLK4 populations treated with the indicated dose of Dox, at the indicated time points. **E -** Representative images of interphase cells containing p53-negative and positive nuclei. **F -** Relative frequency of p53-positive nuclei in MCF10A-PLK4 populations treated with the indicated dose of Dox, at the indicated time points. The bars indicate the average of two independent experiments. Symbols in D and F represent independent experiments. Statistical analyses in D and F were performed using a linear model with relative p53 intensity (by immunoblotting or by immunofluorescence) in a cell as a response variable and taking Dox concentration and time point as independent categorical predictors, plus their interaction. Significant differences between the indicated condition and the one treated with Dox0 at the same time point are indicated with *** (p-value < 0.001).

Centrosomal PLK4 levels were restored in evolved MCF10A-PLK4 populations despite its mRNA levels remaining elevated

In the previous sections, we dissected the processes underlying the fitness cost correlated with increased centriole numbers. This could have occurred by inhibition or loss of PLK4 overexpression, for example through loss of the transgene or hypermethylation of the promoter[57], or inhibition of centriole overproduction.

We asked if the reduction in centriole amplifications could be explained by loss/down-regulation of PLK4 exogenous and/or endogenous expression. We first quantified PLK4 exogenous and endogenous expression by RT-qPCR. In MCF10A-PLK4$^{1\text{-}608}$ populations, the PLK4 transgene was consistently overexpressed (Fig. S7). For MCF10A-PLK4 populations treated with Dox0.001, the levels of the exogenous PLK4 mRNA were not significantly elevated across the experiments (Fig. 7A). This is comparable to previous studies, which showed that small increases in PLK4 mRNA lead to centriole amplification[19,31,58]. Intriguingly, in MCF10A-PLK4 Dox 0.1-treated populations, we observed significant overexpression of the PLK4 transgene at days 1, 3, 46, and 64, but not at days 16 and 31 (Fig. 7A). Then, we measured the expression levels of the endogenous PLK4 gene. Expression levels were not altered in any of the cell lines, Dox concentrations and time points with exception of a decrease in endogenous PLK4 expression in the Dox 0.1 MCF10A-PLK4 population at day 3 (Fig. 7B, S7). We validated these results with a different set of primers targeting the exogenous or both the exogenous and endogenous PLK4 genes, and observed similar results (Fig S7). Thus, the PLK4 transgene was significantly overexpressed at Dox0.1, despite an apparent decrease at days 16 and 31. This suggests that transcriptional silencing may have contributed to the decrease in relative frequency of mitotic cells with extra centrioles at those stages. However, this cannot explain the loss in the capacity of evolved MCF10A-PLK4 populations in Dox0.1 to amplify centrioles at days 46 and 64 (Fig. 2C).

STIL and SAS-6 are two key proteins for proper centriole assembly and their recruitment to the centrosome is dependent on PLK4[29,30,59–61]. Therefore, we asked if downregulation of STIL or SAS-6 could be compensating for PLK4 overexpression. However, we did not observe any significant differences in the expression levels of STIL or SAS-6 in induced versus non-induced MCF10A-PLK4 at any time point (Fig. S8). Thus, the reduction of centriole amplification observed could not be explained by down-regulation of these genes.

Despite PLK4 remaining overexpressed, other regulatory mechanisms could be preventing centriole overproduction, such as inhibition of translation, increase in protein degradation, decrease in kinase activity, or impaired centrosomal recruitment. Thus, we performed immunostaining of PLK4 and measured its levels specifically at the centrosome by immunostaining. For MCF10A-PLK4 populations in Dox0.1 we observed an increase in the centrosomal PLK4 over the first three days, which returned to basal levels at days 31 and 64 (Fig. 7C,D). At days 31 and 64 there were no significant differences between populations grown and the corresponding non-induced populations (Fig. 4D). Thus, PLK4 overexpression levels as measured by RT-qPCR were correlated with an accumulation of centrosomal PLK4 at the first time points. However elevated PLK4 mRNA did not translate into higher levels of PLK4 at the centrosome in the later stages of the experiments. These results suggest that the long-term suppression of centriole amplification could be explained by a reduction in the levels of centrosomal PLK4. Thus, whereas initially centriole amplification is countered by reduced

proliferation of cells with extra centrioles and down-regulation of PLK4 overexpression, at later stages, a different mechanism may block PLK4 biosynthesis or centrosomal recruitment irrespective of high RNA levels.

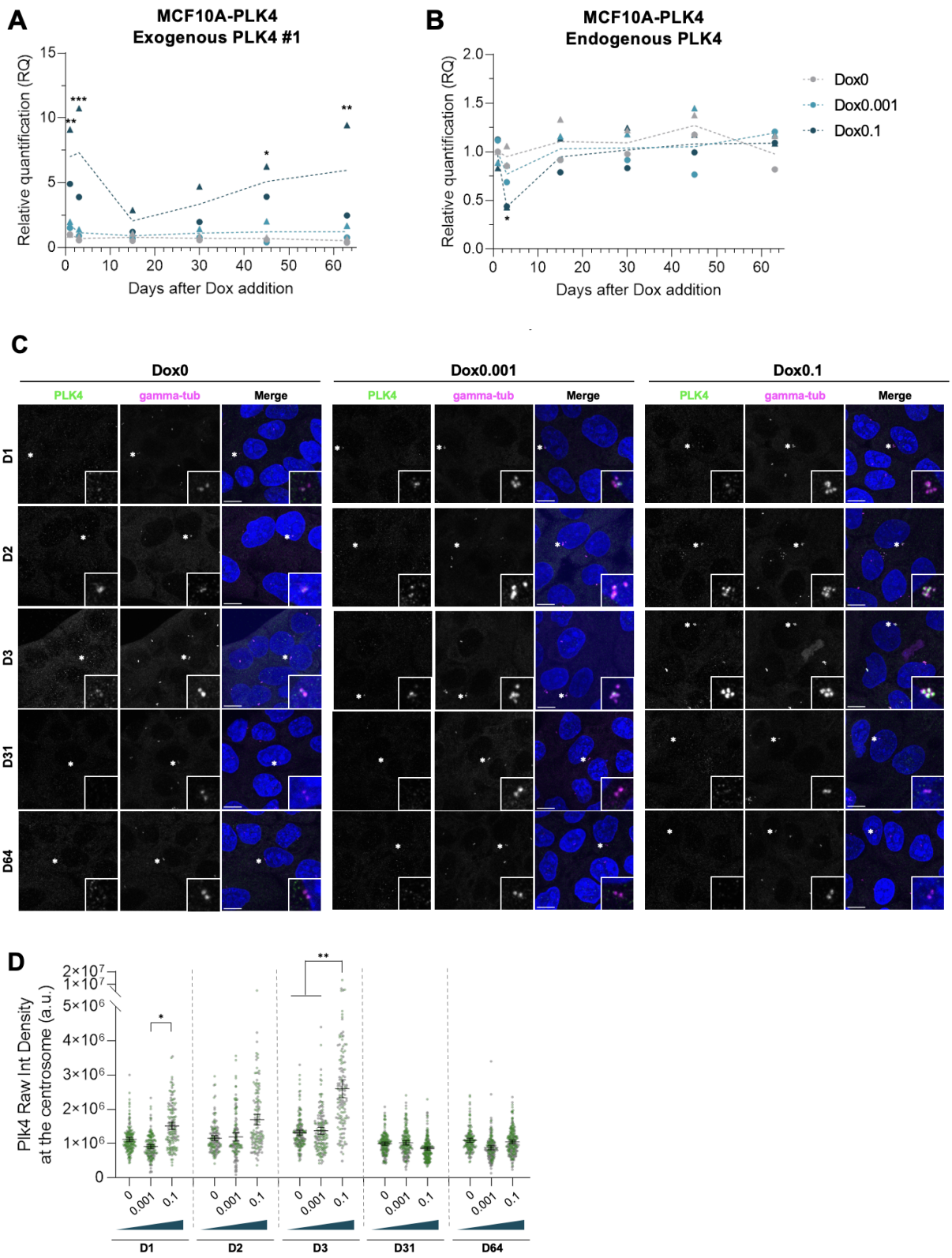

Figure 7: Centrosomal PLK4 levels were restored in evolved MCF10A-PLK4 despite its mRNA levels remaining elevated. A, B - PLK4 mRNA levels analysed by RT-qPCR. The primer sets used are specific for exogenous (A) and endogenous PLK4 (B). Dashed line corresponds to the average RQ in two independent experiments measured in RNA extracted from MCF10A-PLK4 populations grown with Dox0 (grey), Dox0.001 (blue), Dox0.1 (dark blue) µg/mL at the indicated time points. Statistical analyses were performed using linear mixed models taking Dox concentration and day as independent predictors, plus their interaction, and experiment as a random effect, with RQ as a response variable. **C -** Representative image of cells stained for PLK4 (green), gamma-tubulin (magenta) and DNA (blue). **D -** Levels of centrosomal PLK4 in MCF10A-PLK4 populations grown in Dox0, Dox0.001, and Dox0.1 at the indicated time points. 50 to 100 cells were quantified per condition for each of the two independent experiments. Colours (grey and green) represent independent experiments. Statistical analyses were performed using generalised linear models taking Dox concentration and day as independent predictors, plus their interaction, with the natural logarithm of the mean raw integrated density as a response variable. Significant differences between the indicated conditions in A, B, and D and the Dox-0 control at the respective day are represented with * (p-value<0.05), ** (p-value<0.01), and *** (p-value<0.001).

Suppression of centriole amplification in evolved MCF10A-PLK4 populations treated with Dox is irreversible

We showed that loss of centriole amplification was correlated with an increase in relative fitness and reduction in the levels of centrosomal PLK4 despite its continued overexpression, suggesting a long-term inhibition of the production of extra centrioles in MCF10A-PLK4 evolved in Dox0.1 at all Dox levels and in MCF10A-PLK4 evolved in Dox0.001 in 0.001 Dox. This suggests some degree of irreversibility of evolution. So, we next asked if this reduction in centriole amplification capacity was reversible. We cultured evolved MCF10A-PLK4 populations without Dox for 20 days. Then, we treated them with different concentrations of Dox for 24h and analysed centriole numbers. We observed that cell populations that evolved without Dox experienced a dose-dependent increase in the relative frequency of mitotic cells with extra centrioles when they were treated with Dox at 0.001 or 0.1 µg/mL (Fig. 8A Left). In contrast, evolved populations grown with Dox0.001 or 0.1 µg/mL did not show an increase in centriole amplification when treated with those concentrations, respectively (Fig. 8A, Center and Right). Similarly, when as a control, these populations were maintained at the respective concentration of Dox, we observed no significant differences in the relative frequency of mitotic cells with extra centrioles.

Therefore, the repression of centriole amplification in these populations was stable over time despite induction having been relieved. We concluded that chronic Dox treatment induced a potentially irreversible loss in the capacity of MCF10A-PLK4 to generate extra centrioles. Finally, we analysed the level of PLK4 overexpression in these populations (Fig 8B). Treatment with Dox0 and Dox0.001 did not significantly affect the expression of the PLK4 transgene in any condition. In contrast, treatment with Dox0.1 induced significant overexpression of the PLK4 transgene in Dox0.1-evolved populations grown for 20 days with or without Dox, without resulting in centriole amplification. Intriguingly, the Dox0-evolved population grown for 20 days without Dox and treated with Dox0.1 showed a non-significant increase in the expression level of the PLK4 transgene. We observed similar trends of PLK4 expression using a different primer set for the transgenic mRNA and primers targeting both

the exogenous and endogenous PLK4 transcripts. These results suggest that evolved populations were generally less sensitive to induction of PLK4 overexpression by Dox. Moreover, these results might explain the less extreme levels of centriole amplification in Dox0-evolved populations when treated with Dox compared with the ancestral population.

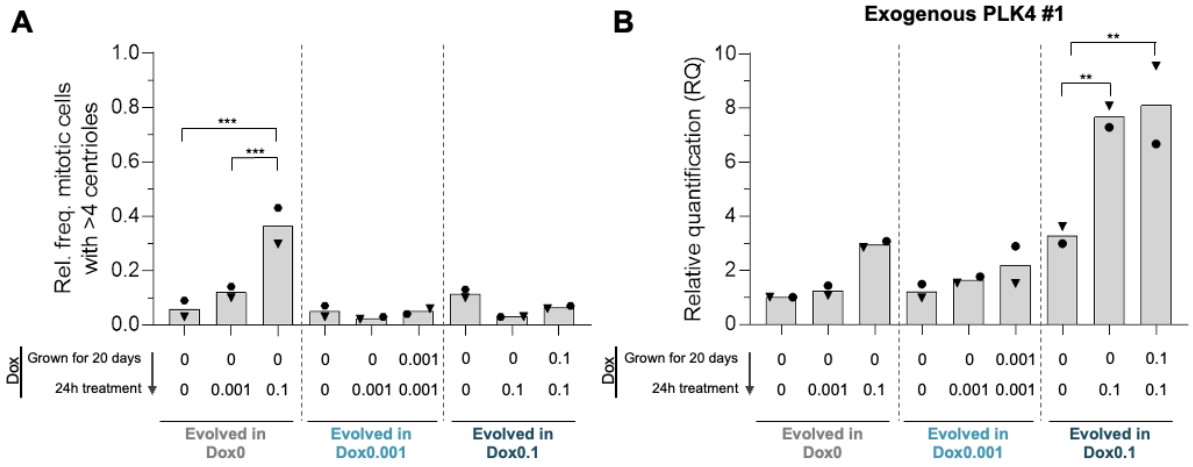

Figure 8: Suppression of centriole amplification in evolved MCF10A-PLK4 populations treated with Dox is irreversible. A - Relative frequency of mitotic cells with more than four centrioles in populations evolved in 0, 0.001 or 0.1 µg/mL of Dox, grown for additional 20 days without Dox and treated with the indicated doses of Dox for 24h. As controls, cells were grown in parallel with the same dose of Dox as during experimental evolution. At least 50 cells were analysed per condition for each of the two independent experiments. Symbols represent independent experiments. **B** - PLK4 mRNA levels analysed by RT-qPCR. The primer sets used are specific for exogenous (PLK4 (B). Dashed line corresponds to the average RQ in two independent experiments measured in RNA extracted from MCF10A-PLK4 populations grown with Dox at 0 (grey), 0.001 (blue), and 0.1 (dark blue) µg/mL at the indicated time points.

Discussion

In this study, we conducted the first systematic assessment of how cell populations evolve in response to different levels of centriole amplification induced by chronic PLK4 overexpression. More specifically, we quantified fitness, cell proliferation, centriole numbers, and PLK4 dynamics and how these parameters correlate and change over time. We showed that MCF10A-Plk4 populations that evolved under chronic PLK4 overexpression inhibited centriole amplification in a dose-dependent way. We observed a fitness cost associated with slower proliferation, cell cycle alterations, and p53 activation that was proportional to the level of centriole amplification. Adaptation to chronic PLK4 overexpression depended on the level of centriole amplification, with populations evolved at a low concentration of Dox retaining the capacity to amplify centrioles when treated with higher concentrations, whereas cells evolved at higher Dox were irreversibly blocked from responding. Cells initially responded to high chronic induction by down-regulating PLK4 overexpression. This was followed by a long-term response that was independent of PLK4 transcriptional regulation but prevented the accumulation of excess PLK4 at the centrosome. In summary, our work is indicative of a dose-dependent, two-step response to chronic PLK4 overexpression that reduces long-term centriole amplification.

Centriole number dynamics and the role of selection

Several studies have looked into the effect of transiently or chronically overexpressing PLK4, but they were focused on a short window of time, not allowing for a complete understanding of the potential factors that can regulate centriole number dynamics over long periods of time, as it occurs in cancer. The centriole number dynamics we observed following chronic PLK4 overexpression are reminiscent of those previously reported following transient centriole numbers perturbations[10,22–25]. In brief, the initial distribution of centriole numbers per cell was recovered following transient centriole number increases, as we observed following chronic PLK4 overexpression. However, our results differ in a few key aspects. First, the dynamics of centriole number loss in our populations were significantly slower than those reported in other studies. Whereas centriole number increases following PLK4 overexpression or treatment with cytokinesis-blocking drugs were resolved within 12 days in RPE[10] or RPE p53-KO[24] cell lines, respectively, in our experimental setup, populations showed elevated levels of centriole amplification for up to 46 days of chronic PLK4 overexpression. Secondly, whereas negative selection against cells bearing supernumerary centrioles appears sufficient to govern centriole number dynamics following transient perturbation[10], our results indicate that that is insufficient for explaining the long-term dynamics as cells continue to express high PLK4 mRNA levels. Our results highlight a more complex form of overproduction-selection balance in these conditions than what was previously reported following transient centriole number alterations.

Although centriole amplification is widely regarded as deleterious, it is not known if the number of extra centrioles aggravates these effects. We previously inferred that in many cell lines, selection acts uniformly regardless of the number of extra centrioles per cell[26]. In other words, population fitness may depend on the relative frequency of cells with centriole amplification. regardless of the number of extra centrioles they contain. Since the relative frequency of cells with centriole amplification and mean centriole number are correlated in our experiments, we

could not verify this prediction experimentally, although the former was a better predictor of fitness.

Loss of centriole amplification in previous studies was attributed to p53 limiting the growth of cells with extra centrioles[6,36]. However, we did not observe p53 activation in the evolved populations. This suggests other mechanisms may be responsible for suppressing chronic centriole amplification. It is possible that p53 merely delays the decrease in the number of cells with extra centrioles rather than enabling chronic centriole amplification. In the future, it would be interesting to perform experimental evolution of p53-null cells and assess how centriole number dynamics differ in that case.

Adaptation to chronic PLK4 overexpression involved a two-step regulatory process

Aside from selection, the short-term response to centriole amplification was characterised by down-regulation of PLK4, which probably decreased the rate of centriole overproduction. Importantly, another study also reported a reduction in PLK4 mRNA abundance in mouse embryonic fibroblasts following chronic centriole amplification over short time periods, though this was not followed up[19]. However, at later time points, we observed that PLK4 was overexpressed at similar levels to the initial condition, despite the absence of significant centriole amplification. Similarly, it was previously observed *in vivo* that several tissues showed elevated PLK4 mRNA levels following chronic induction despite lacking centriole amplification, although the authors did not track these dynamics[19]. Our results reconcile these two observations, and we propose that chronic PLK4 overexpression triggers a two-step regulatory response.

Notwithstanding, it was not known how long-term PLK4 overexpression affected protein abundances at the centrosome. Here, we showed that PLK4 did not over-accumulate at the centrosome in evolved populations, despite increased mRNA levels. This suggests that some mechanism downstream of transcription, possibly at the level of protein degradation or recruitment inhibits centriole overproduction. Mutations in the PLK4 transgene are unlikely to explain the results at Dox 0.001 since we observed centriole amplification in the populations evolved in Dox0.001 when treated with higher Dox concentration to a similar extent as the population evolved in Dox0. Given that the ability to generate extra centrioles did not revert after 20 days of growth without Dox, this mechanism should be heritable. Identifying its molecular underpinnings, including how long it can be sustained, might help understanding of how centriole amplification is maintained in cancer. Moreover, if the molecular mechanism of adaptation depends on changes in other molecules besides PLK4, those alterations could potentially be an Achilles heel of tumours that overexpress PLK4.

Whereas our data seem to indicate that the alterations observed in induced MCF10A-PLK4 populations are due to elevated centriole numbers, by comparison with control MCF10A-PLK4$^{1-608}$, it is pertinent to note that our study does not completely rule out that our results may be specific of PLK4 overexpression. In the future, it will be important to conduct additional experiments chronically overexpressing other centriolar genes, such as (e.g. STIL or SAS-6),

to better clarify the role of centriole amplification in cellular evolution. These approaches will be important to assess if there are common adaptive mechanisms to centriole overproduction or if these responses are protein-specific.

Implications for cancer cell biology

Our measurements of the competitive index showed that populations with low levels of centriole amplification imparted a less severe fitness cost. This suggests that cells displaying a phenotype which leads to modest centriole amplification, i.e. some cells produce extra centrioles and others contain wild-type centriole numbers, can potentially escape selection purely by chance. If that is the case, mechanisms that render cells more tolerant to centriole amplification might not be necessary to maintain cells with extra centrioles in cancer. On the other hand, it might be necessary to disrupt mechanisms that regulate centriole overproduction in order to sustain chronic centriole amplification.

We showed that adaptation to chronic PLK4 overexpression was partly due to the inhibition of centriole amplification. Unlike what is commonly observed in experimental evolution, for example, with respect to antibiotic resistance[52], we observed no cost of adaptation to Dox treatment. Thus, temporary centriole amplification, despite its known role in generating aneuploidies, did not seem to affect the evolution of these populations with respect to their general capacity to proliferate. It was previously proposed that low levels of centriole amplification are pro-tumorigenic whereas high levels of centriole amplification do not favour tumour formation[19]. This implies that low levels of centrosome amplification can be retained for longer periods of time and/or accelerate cancer evolution, for instance, by generating less severe aneuploidies, compared with high levels of centrosome amplification. Whereas our results indicate that low levels of centriole amplification are better tolerated, which would support this idea, the populations that evolved did not outcompete the ancestral populations without Dox. It would be interesting to assess the fitness of these populations in other scenarios; for example, in the presence of drugs used in cancer treatment or within the context of the tumour in the animal.

Centriole amplification has been associated with non-cell-autonomous promotion of invasion and migration[11,12] in MCF10A cells in 3D culture setups. Our results indicate that centriole amplification does not affect the growth dynamics of other cells in the population. As cell proliferation depends on the physical interactions between cells in a population, it would be interesting to test if centriole amplification may affect proliferation of neighbouring cells in 3D cultures and also *in vivo.*

Centriole number is known to vary along cancer progression[18]. The source of these changes remains poorly understood but is usually attributed to gene expression changes or genetic mutations. Interestingly, we observed that the response of the evolved populations was tailored to the level of PLK4 overexpression they experienced. Whereas populations evolved under high levels of chronic PLK4 overexpression suffered irreversible inhibition of centriole amplification, populations evolved under low levels of chronic PLK4 overexpression remained permissive to centriole amplification when challenged with stronger induction. Our results indicate that cells capable of centriole amplification are not necessarily eliminated from the

population and remain sensitive to higher levels of PLK4 overexpression. This may explain how extra centrioles are maintained in cancer, and how their numbers may vary along disease progression. Furthermore, several cancer types are known to overexpress PLK4, being an attractive therapeutic target, for which drugs have been developed[62]. Our work suggests that there is a mechanism that allows PLK4-overexpressing cells to evade chronic centriole amplification. Targeting this mechanism in tumours that overexpress PLK4 could be an interesting therapeutic strategy for potentially selectively eliminating these cells.

Acknowledgements

We thank Susana Godinho for sharing the cell lines. We thank the support of IGC's Advanced Imaging Unit (AIU), especially Alexandre Lopes, Patrícia Rodrigues and Gabriel Martins, funded by PPBI-POCI-01-0145-FEDER-022122 (Lisboa 2020/FEDER/FCT; Portugal); Flow Cytometry Unit, especially Marta Monteiro, and Advanced Data Analysis Unit, for their support in this work. We thank Luca Fava for critical reading of this manuscript and Stephan Peischel for discussion of statistical analyses. We also thank the CCR and ED/THEE labs for their continued support and discussion of this work. This work was supported by the European Research Council (ERC CoG 683528 to M.B.D. and ERC StG 804569 to C.B.) and FCT PhD fellowships awarded to M.L. and C.P. (PD/BD/139217/2028 and PD/BD/128004/2016, respectively).

Author contributions

M.A.D.L. and C.P. designed and performed all experiments, except for the ones listed below, and discussed all analyses. M.A.D.L. performed centriole number quantifications, quantification of p53 by immunostaining, flow cytometry data acquisition, and all statistical analyses. C.P. performed PLK4 immunostaining and analysis, p53 immunostaining, p53 Western blotting and analysis, and RT-qPCR and analysis. M.A.D.L., C.P. and M.B.D. critically discussed experimental results. M.A.D.L., C.P., C.B., and M.B.D conceptualised the study. M.A.D.L. and C.P wrote the manuscript. C.B. and M.B.D. edited the manuscript. M.A.D.L. and C.P. contributed equally for this work.

Declaration of interests

The authors declare no conflict of interest.

Methods

Cell culture

We cultured MCF10A-TetR, MCF10A-PLK4$^{1-608}$, and MCF10A-PLK4 as described previously[11]. We cultured the cells in DMEM (Gibco) and F-12 (Gibco) at 1:1 ratio, supplemented with horse serum at 5%, L-glutamine (Thermo Scientific) at 0.5 μg/mL, penicillin and streptomycin (Thermo Scientific) at 100 U/mL, insulin (Sigma) at 10 μg/mL, hydrocortisone (Sigma) at 100 ng/mL, cholera toxin (Sigma) at 1 μg/mL, epidermal growth factor (Sigma) at 20 ng/mL, and maintained them at 37◦ C in a 5% CO_2 atmosphere. All cell lines were tested for the presence of mycoplasma.

For the evolution experiment, we passaged cells every 72h and subcultured them in 150 mm dishes ensuring that cells were sub-confluent at the time of passaging, such that they predominantly spent time in exponential growth. The medium for doxcycyline-treated populations was further supplemented with doxycycline to a final concentration of 0.001 or 0.1 μg/mL. During passaging, cells were counted using a Scepter 2.0 Handheld Automated Cell Counter (Merck Millipore) and 60 μm Sensors (Merck Millipore). The growth rate of each condition was calculated taking the number of cells at passaging, N_{pass}, and the initial seeding cell number, N_{seed}, which we fixed at 2.2x10^6 cells, according to:

$$N_{pass}=N_{seed}\, e^{r(t\_pass-t\_seed)}$$

where r is the exponential growth rate (per day), t_pass is the day of passaging, and t_seed is the day when the population was seeded. Relative growth rates were then obtained by taking the growth rate for a given condition, at a given time point t_pass, and dividing it by the growth rate of the Dox0-treated population of the same cell line at the respective time point.

Competition assays and flow cytometry

We seeded 1.5x10^6 cells at days -1, 29, and 62 of each experimental evolution replicate in two T-25 flasks per condition, such that confluency was not reached in the next day and cells maintained exponential growth. At day 0 of each competition assay, CellTrace CFSE (Thermo Scientific) or CellTrace Far Red (Thermo Scientific) staining was performed according to manufacturer instructions. In brief, we replaced the cell culture medium in the flasks with 3 mL of 10 μM CellTrace CFSE or 2 μM CellTrace Far Red in PBS and incubated the cells at 37ºC for 20 minutes. After staining, we washed the flasks with an equal volume of medium supplemented with 5% horse serum to remove unbound dye molecules. Then, we detached, centrifuged and resuspended the cells in the corresponding media. Co-cultures were prepared by mixing populations stained with CellTrace CFSE and CellTrace Far Red at 1:1 ratio. We seeded monocultures and co-cultures such that the confluency at the time of harvest was approximately 70-80%. At days 1 through to 3, cells were stained with 5 μg/mL Hoechst 33342 (Invitrogen) in cell culture medium for 30 minutes at 37ºC, before detaching them. Finally, we resuspended the cells in 1 μg/mL propidium iodide (PI, Sigma) staining solution and incubated them at 37ºC for 10 minutes. Mono- and/or co-cultures were then analysed by flow cytometry.

Flow cytometry analysis was conducted using a BD Fortessa X-20 cytometer and BD FACSDiva software. The cell population was gated based on their forward- and side-scatter

area parameters (FSC-A and SSC-A, respectively) and doublets were excluded by plotting the area against the width of the forward-scatter parameter. Exclusion of dead cells was performed by gating out PI-positive cells. Finally, we gated live single-positive CellTrace CFSE and CellTrace FarRed cells for competition, proliferation analysis, and cell cycle analysis. Live cells in each cell cycle stage were manually gated. For viability analysis, we identified CellTrace CFSE- and CellTrace Far Red-positive singlets and excluded PI-positive cells in each sub-population. We acquired approximately 20,000 live cells for each sample during the evolution experiment and around 10,000 live cells for the remaining competition assays. Flow cytometry data was analysed using FlowJo.

Quantification of competitive index, and dye decay rate

As mentioned in the previous section, we first gated single-positive CellTrace CFSE and CellTrace Far Red populations. We observed a small population of double-positive cells, as reported in the literature, which we excluded from further analysis. The relative frequency, p, of each sub-population labelled with each dye i, at day t was calculated according to the following expressions:

$$p_{FarRed}(t) = N_{CFSE}(t) \,/\, (N_{CFSE}(t) + N_{FarRed}(t))$$

where $N_i(t)$ is the total number of single-positive cells for CellTrace CFSE or CellTrace Far Red. As a proxy for fitness, we employed the competitive index, given by:

$$w = \ln(p_{CFSEi}(3) \,/\, p_{FarRed}(3) \,/\, p_{CFSE}(1) \,/\, p_{FarRed}(1))$$

To calculate the mean rate of dye decay, as a proxy for the mean cell division rate, we first computed the average CFSE/Far Red intensity in single-positive cells at each day of the competition assay. As above, double-positive cells were excluded. As a simplification, we assumed constant dye decay and estimated the mean decay rate by performing a linear regression on the logarithm of the differences of average dye intensity.

Estimation of competitive index and mean dye decay rate was performed using R.

Immunofluorescence and microscopy

For staining and imaging of centriolar proteins, cells were grown on 13 mm coverslips in 24-well plates, using the appropriate cell culture medium and fixed with 100% methanol at -20ºC for 10 minutes. For immunostaining, we started by incubating cells with blocking solution (10% FBS in 1X PBS) for 30 minutes at room temperature. Samples were incubated with primary antibody dilutions (prepared in blocking solution) for 1 hour at room temperature or overnight at 4ºC. Cells were then washed with 1X PBS and incubated with secondary antibody dilutions for 1 hour at room temperature. DNA staining was performed by incubating the cells with 1 μg/mL Hoechst 33342 for 15 minutes at room temperature. Alternatively, cells were stained with DAPI during secondary antibody incubation. For immunostaining of p53, cells were incubated with a solution containing the p53 primary antibody and nanobody which were

previously incubated together for 1 hour at room temperature, prepared according to manufacturer instructions. Finally, we mounted coverslips on microscopy slides, using Vectashield mounting medium (Vector Laboratories). Primary antibodies used: anti-CEP135 1:500 (rabbit, Abcam), anti-Centrin 1:500 (mouse, clone 20H5, Millipore); anti-PLK4 1:500 (rabbit, Metabion REF paper), anti-p53 1:500 (mouse, Millipore), anti-gamma-tubulin (mouse, clone GTU88, Sigma). Secondary antibodies used were: goat/donkey anti-mouse Alexa Fluor 488 1:500 (Molecular Probes), donkey anti-rabbit Rhodamine Red 1:500 (Jackson Immunireasearch), donkey anti-rat Alexa Fluor 647 (Molecular Probes). Nanobody (Atto 542 FluoTag-X2 anti-Mouse Kappa light chain, Nanotag). Images of mitotic cells for assessing centriole numbers and interphase cells for quantification of PLK4 levels and nuclear p53 were acquired using an Eclipse Ti-2 inverted microscope with 3i Marianas spinning-disk using a 100X objective and Andor Dragonfly spinning-disk, respectively.

Image analysis

Microscopy images were analysed using Fiji/ImageJ. Centriole number counting was performed on 3D stacks. Each Centrin focus co-localising with a CEP135 focus was scored as a centriole. To assess centrosomal PLK4 levels, we applied a threshold (Triangle) in the gamma-tubulin channel to define ROI corresponding to the centrosome. Then, we used these ROI to measure PLK4 intensity (Raw Integrated Density) in its sum projections. To quantify presence/absence of nuclear p53, we adjusted the histograms of the p53 channel to a fixed range in order to compare between images and scored p53-positive nuclei.

Western blotting

Cells lysis was performed by incubating cells in lysis buffer (Tris 10 mM pH7.4, EDTA 5 mM, NaCl 100 mM, Triton X-100 1%, Na3VO4 0,2 mM, NaF 50 mM, DTT 1 mM, Protease inhibitors (Roche)) on ice for 30 min. Then, samples were centrifuged at 13 500 rpm for 15 min at 4ºC and the supernatant was transferred to a new tube. Protein extracts were quantified using the Bradford method and 60 μg of total protein (per sample) were run and separated on sodium dodecyl sulphate-polyacrylamide gel electrophoresis (SDS-PAGE) and transferred onto nitrocellulose membranes. For western blotting, the membranes were blocked with 5% milk in TBS 1X, following incubation with the primary antibodies anti-p53 (1:500, mouse, (Ab-6) Pantropic OP43 Sigma-Aldrich) and anti-GAPDH (1:1000, rabbit, 14C10 Cell Signaling) for 1h at room temperature. Then, membranes were washed with TBS 1X, incubated with secondary antibodies IRDye 800CW Goat anti-Mouse (1:10 000, #926-32210, Li-cor) and IRDye 680RD Goat anti-Rabbit (1:10 000, #926-68071, Li-cor) for 1h at room temperature. Membranes were then washed and developed in Odyssey (Li-cor). Band intensity was quantified using Fiji/ImageJ.

RNA extraction and RT-qPCR

RNA extraction was performed using the RNeasy Mini Kit (Qiagen) according to manufacturer instructions. For each sample, we performed on-column DNA digestion using RNase-free

DNAse (Qiagen) as specified by the kit. RNA quantity and purity were assessed using NanoDrop 2000 (Thermo Scientific). We performed cDNA synthesis using the High Capacity RNA-to-cDNA kit (Applied Biosystems), according to manufacturer instructions.

For the RT-qPCR reactions we used iTaq SYBR Green (BioRad) according to kit instructions. Samples were prepared in triplicate in 384-well plates. The qPCR run and data analysis were performed using QuantStudio (Applied Biosystems). The following primers were used for quantifying the mRNA levels of GAPDH, exogenous PLK4 *truncated or full-length), endogenous PLK4, total PLK4 (i.e. primers anneal to both the exogenous and endogenous sequences), STIL, and SAS-6.

Target	Sequence	Orientation	Reference
GAPDH #1	5′ -TTAAAAGCAGCCCTGGTGAC-3′	Forward	Godinho et al. 2014[11]
GAPDH #1	5′ -CTCTGCTCCTCCTGTTCGAC-3′	Reverse	Godinho et al. 2014[11]
GAPDH #2	5′-ACATCGCTCAGACACCATG-3′	Forward	Cabrera *et al.* 2018[63]
GAPDH #2	5′ -TGTAGTTGAGGTCAATGAAGGG-3′	Reverse	Cabrera *et al.* 2018[63]
Exogenous PLK4 #1	5′-TTTCCGAGGAGGATTTGCCC-3′	Forward	This paper
Exogenous PLK4 #1	5′ -ACCAGTGTGAATGGACTCAGC-3′	Reverse	This paper
Exogenous PLK4 #2	5′-CAGGATTTGCCCGGGATGGCG-3′	Forward	Godinho et al. 2014[11]
Exogenous PLK4 #2	5′-AACCAGTGTGAATGGACTCAGCTCT-3′	Reverse	Godinho et al. 2014[11]
Endogenous PLK4	5′-CTAATCCGGAGAACCCAGGC-3′	Forward	This paper
Endogenous PLK4	5′ -ACCAGTGTGAATGGACTCAGC-3′	Reverse	This paper

Total PLK4	5′-AGACCACCCTTCGACACTGA-3′	Forward	Sala *et al.* 2020[10]
Total PLK4	5′ -GTCCTTGGCCTCTATTGACAAA-3′	Reverse	Sala *et al.* 2020
STIL	5′-AATGAAGTCACAAGTCTTCCAGG-3′	Forward	This paper
STIL	5′ -CACAACTAGAGAAGAGCTGTTGG-3′	Reverse	This paper
SAS-6	5′ -GAATGGGCGTCACATACAGC-3′	Forward	This paper
SAS-6	5′ -TTGATATTGAACCTGTGCCTGC-3′	Reverse	This paper

Data visualisation and statistical analyses

Plots were produced using Graphpad Prism. Statistical analyses were performed in R and Graphpad Prism.

References

1. Brito DA, Gouveia SM, Bettencourt-Dias M. Deconstructing the centriole: Structure and number control. Current Opinion in Cell Biology. 2012;24(1):4–13. doi:10.1016/j.ceb.2012.01.003
2. Gönczy P. Centrosomes and cancer: Revisiting a long-standing relationship. Nature Reviews Cancer. 2015;15(11):639–652. http://www.nature.com/doifinder/10.1038/nrc3995. doi:10.1038/nrc3995
3. Breslow DK, Holland AJ. Mechanism and Regulation of Centriole and Cilium Biogenesis. Annual Review of Biochemistry. 2019;88(1):691–724. doi:10.1146/annurev-biochem-013118-111153
4. Gomes Pereira S, Dias Louro MA, Bettencourt-Dias M. Biophysical and Quantitative Principles of Centrosome Biogenesis and Structure. Nature Communications. 2021;37:43–63. doi:10.1038/s41467-017-00238-8.
5. Nabais C, Peneda C, Bettencourt-Dias M. Evolution of centriole assembly. Current Biology. 2020;30(10):R494–R502. doi:10.1016/j.cub.2020.02.036
6. Holland AJ, Fachinetti D, Zhu Q, Bauer M, Verma IM, Nigg EA, Cleveland DW. The autoregulated instability of Polo-like kinase 4 limits centrosome duplication to once per cell cycle. Genes Dev. 2012;26(24):2684–2689.
7. Kwon M, Godinho SA, Chandhok NS, Ganem NJ, Azioune A, Thery M, Pellman D. Mechanisms to suppress multipolar divisions in cancer cells with extra centrosomes. Genes and Development. 2008;22(16):2189–2203. doi:10.1101/gad.1700908
8. Ganem NJ, Godinho SA, Pellman D. A mechanism linking extra centrosomes to chromosomal instability. Nature. 2009;460(7252):278–282. http://www.nature.com/doifinder/10.1038/nature08136. doi:10.1038/nature08136
9. Cosenza MR, Cazzola A, Rossberg A, Schieber NL, Konotop G, Bausch E, Slynko A, Holland-Letz T, Raab MS, Dubash T, et al. Asymmetric Centriole Numbers at Spindle Poles Cause Chromosome Missegregation in Cancer. Cell Reports. 2017;20(8):1906–1920. https://www.sciencedirect.com/science/article/pii/S2211124717310768. doi:https://doi.org/10.1016/j.celrep.2017.08.005
10. Sala R, Farrell KC, Stearns T. Growth disadvantage associated with centrosome amplification drives population-level centriole number homeostasis. Molecular Biology of the Cell. 2020:mbc.E19–04–0195. doi:10.1091/mbc.e19-04-0195
11. Godinho SA, Picone R, Burute M, Dagher R, Su Y, Leung CT, Polyak K, Brugge JS, Théry M, Pellman D. Oncogene-like induction of cellular invasion from centrosome amplification. Nature. 2014;510(7503):167–171. doi:10.1038/nature13277
12. Arnandis T, Monteiro P, Adams SD, Bridgeman VL, Rajeeve V, Gadaleta E, Marzec J, Chelala C, Malanchi I, Cutillas PR, et al. Oxidative Stress in Cells with Extra Centrosomes Drives Non-Cell-Autonomous Invasion. Developmental Cell. 2018;47(4):409–424.e9. doi:10.1016/j.devcel.2018.10.026
13. Adams SD, Csere J, D'angelo G, Carter EP, Romao M, Arnandis T, Dodel M, Kocher HM, Grose R, Raposo G, et al. Centrosome amplification mediates small extracellular vesicle secretion via lysosome disruption. Current Biology. 2021;31(7):1403-1416.e7. doi:10.1016/j.cub.2021.01.028
14. Chan JY. A clinical overview of centrosome amplification in human cancers. Int. J. Biol. Sci. 2011;7(8):1122–1144.

15. Bettencourt-Dias M, Hildebrandt F, Pellman D, Woods G, Godinho SA. Centrosomes and cilia in human disease. Trends in Genetics. 2011;27(8):307–315. doi:10.1016/j.tig.2011.05.004
16. Godinho SA, Pellman D. Causes and consequences of centrosome abnormalities in cancer. Philosophical Transactions of the Royal Society B: Biological Sciences. 2014;369(1650). doi:10.1098/rstb.2013.0467
17. Denu RA, Zasadil LM, Kanugh C, Laffin J, Weaver BA, Burkard ME. Centrosome amplification induces high grade features and is prognostic of worse outcomes in breast cancer. BMC Cancer. 2016;16(1). doi:10.1186/s12885-016-2083-x
18. Lopes CAM, Mesquita M, Cunha AI, Cardoso J, Carapeta S, Laranjeira C, Pinto AE, Pereira-Leal JB, Dias-Pereira A, Bettencourt-Dias M, et al. Centrosome amplification arises before neoplasia and increases upon p53 loss in tumorigenesis. Journal of Cell Biology. 2018;217(7):2353–2363. https://doi.org/10.1083/jcb.201711191. doi:10.1083/jcb.201711191
19. Levine MS, Bakker B, Boeckx B, Moyett J, Lu J, Vitre B, Spierings DC, Lansdorp PM, Cleveland DW, Lambrechts D, et al. Centrosome Amplification Is Sufficient to Promote Spontaneous Tumorigenesis in Mammals. Developmental Cell. 2017;40(3):313–322.e5. http://dx.doi.org/10.1016/j.devcel.2016.12.022. doi:10.1016/j.devcel.2016.12.022
20. Shoshani O, Bakker B, de Haan L, Tijhuis AE, Wang Y, Kim DH, Maldonado M, Demarest MA, Artates J, Zhengyu O, et al. Transient genomic instability drives tumorigenesis through accelerated clonal evolution. Genes Dev. 2021;35(15–16):1093–1108.
21. Marteil G, Guerrero A, Vieira AF, De Almeida BP, Machado P, Mendonça S, Mesquita M, Villarreal B, Fonseca I, Francia ME, et al. Over-elongation of centrioles in cancer promotes centriole amplification and chromosome missegregation. Nature Communications. 2018;9(1). doi:10.1038/s41467-018-03641-x
22. Wong YL, Anzola J V, Davis RL, Yoon M, Motamedi A, Kroll A, Seo CP, Hsia JE, Kim SK, Mitchell JW, et al. Reversible centriole depletion with an inhibitor of Polo-like kinase 4. Science. 2015;348(6239):1155–1160. http://www.ncbi.nlm.nih.gov/pubmed/25931445%5Cnhttp://www.sciencemag.org/content/348/6239/1155.full.pdf. doi:10.1126/science.aaa5111
23. Lambrus BG, Uetake Y, Clutario KM, Daggubati V, Snyder M, Sluder G, Holland AJ. P53 protects against genome instability following centriole duplication failure. Journal of Cell Biology. 2015;210(1):63–77. doi:10.1083/jcb.201502089
24. Baudoin NC, Nicholson JM, Soto K, Martin O, Chen J, Cimini D. Asymmetric clustering of centrosomes defines the early evolution of tetraploid cells. eLife. 2020;9. doi:10.7554/eLife.54565
25. Galofré C, Asensio E, Ubach M, Torres IM, Quintanilla I, Castells A, Camps J. Centrosome reduction in newly-generated tetraploid cancer cells obtained by separase depletion. Scientific Reports. 2020;10(1). doi:10.1038/s41598-020-65975-1
26. Dias Louro MA, Bettencourt-Dias M, Bank C. Patterns of selection against centrosome amplification in human cell lines. PLOS Computational Biology. 2021;17(5):1–22. https://doi.org/10.1371/journal.pcbi.1008765. doi:10.1371/journal.pcbi.1008765
27. Bettencourt-Dias M, Rodrigues-Martins A, Carpenter L, Riparbelli M, Lehmann L, Gatt MK, Carmo N, Balloux F, Callaini G, Glover DM. SAK/PLK4 is required for centriole duplication and flagella development. Current Biology. 2005;15(24):2199–2207. doi:10.1016/j.cub.2005.11.042
28. Kleylein-Sohn J, Westendorf J, Le Clech M, Habedanck R, Stierhof Y-D, Nigg EA. Plk4-Induced Centriole Biogenesis in Human Cells. Developmental Cell. 2007;13(2):190–202.

https://www.sciencedirect.com/science/article/pii/S1534580707002638. doi:https://doi.org/10.1016/j.devcel.2007.07.002
29. Strnad P, Leidel S, Vinogradova T, Euteneuer U, Khodjakov A, Gönczy P. Regulated HsSAS-6 Levels Ensure Formation of a Single Procentriole per Centriole during the Centrosome Duplication Cycle. Developmental Cell. 2007;13(2):203–213. doi:10.1016/j.devcel.2007.07.004
30. Arquint C, Sonnen KF, Stierhof Y-D, Nigg EA. Cell-cycle-regulated expression of STIL controls centriole number in human cells. Journal of Cell Science. 2012;125(5):1342–1352. doi:10.1242/jcs.099887
31. Lopes CAM, Jana SC, Cunha-Ferreira I, Zitouni S, Bento I, Duarte P, Gilberto S, Freixo F, Guerrero A, Francia M, et al. PLK4 trans-Autoactivation Controls Centriole Biogenesis in Space. Developmental Cell. 2015;35(2):222–235. doi:10.1016/j.devcel.2015.09.020
32. Normand G, King RW. Understanding cytokinesis failure. Adv. Exp. Med. Biol. 2010;676:27–55.
33. Bloomfield M, Cimini D. The fate of extra centrosomes in newly formed tetraploid cells: should I stay, or should I go? Frontiers in Cell and Developmental Biology. 2023;11. https://www.frontiersin.org/articles/10.3389/fcell.2023.1210983. doi:10.3389/fcell.2023.1210983
34. Ogden A, Rida PCG, Aneja R. Prognostic value of CA20, a score based on centrosome amplificationassociated genes, in breast tumors. Scientific Reports. 2017;7(1). doi:10.1038/s41598-017-00363-w
35. De Almeida BP, Vieira AF, Paredes J, Bettencourt-Dias M, Barbosa-Morais NL. Pan-cancer association of a centrosome amplification gene expression signature with genomic alterations and clinical outcome. PLoS Computational Biology. 2019;15(3). doi:10.1371/journal.pcbi.1006832
36. Vitre B, Holland AJ, Kulukian A, Shoshani O, Hirai M, Wanga Y, Maldonado M, Cho T, Boubaker J, Swing DA, et al. Chronic centrosome amplification without tumorigenesis. Proceedings of the National Academy of Sciences of the United States of America. 2015;112(46):E6321–E6330. doi:10.1073/pnas.1519388112
37. Serçin Ö, Larsimont JC, Karambelas AE, Marthiens V, Moers V, Boeckx B, Le Mercier M, Lambrechts D, Basto R, Blanpain C. Transient PLK4 overexpression accelerates tumorigenesis in p53-deficient epidermis. Nature Cell Biology. 2016;18(1):100–110. doi:10.1038/ncb3270
38. Kulukian A, Holland AJ, Vitrec B, Naika S, Cleveland DW, Fuchsa E. Epidermal development, growth control, and homeostasis in the face of centrosome amplification. Proceedings of the National Academy of Sciences of the United States of America. 2015;112(46):E6311–E6320. doi:10.1073/pnas.1518376112
39. Chan JY. A clinical overview of centrosome amplification in human cancers. Int. J. Biol. Sci. 2011;7(8):1122–1144.
40. Ogden A, Rida PCG, Aneja R. Prognostic value of CA20, a score based on centrosome amplificationassociated genes, in breast tumors. Scientific Reports. 2017;7(1). doi:10.1038/s41598-017-00363-w
41. Neben K, Glesecke C, Schweizer S, Ho AD, Krämer A. Centrosome aberrations in acute myeloid leukemia are correlated with cytogenetic risk profile. Blood. 2003;101(1). doi:10.1182/blood-2002-04-1188
42. Arnandis T, Monteiro P, Adams SD, Bridgeman VL, Rajeeve V, Gadaleta E, Marzec J, Chelala C, Malanchi I, Cutillas PR, et al. Oxidative Stress in Cells with Extra Centrosomes

Drives Non-Cell-Autonomous Invasion. Developmental Cell. 2018;47(4):409–424.e9. doi:10.1016/j.devcel.2018.10.026
43. Moreno-Marin N, Marteil G, Fresmann NC, de Almeida BP, Dores K, Fragoso R, Cardoso J, Pereira-Leal JB, Barata JT, Godinho S, et al. High prevalence and dependence of centrosome clustering in mesenchymal tumors and leukemia. bioRxiv. 2023. https://www.biorxiv.org/content/early/2023/03/17/2023.03.13.532472. doi:10.1101/2023.03.13.532472
44. Heinz N, Hennig K, Loew R. Graded or threshold response of the tet-controlled gene expression: All depends on the concentration of the transactivator. BMC Biotechnology. 2013;13. doi:10.1186/1472-6750-13-5
45. Kawecki TJ, Lenski RE, Ebert D, Hollis B, Olivieri I, Whitlock MC. Experimental evolution. Trends in Ecology and Evolution. 2012;27(10):547–560. doi:10.1016/j.tree.2012.06.001
46. Ahler E, Sullivan WJ, Cass A, Braas D, York AG, Bensinger SJ, Graeber TG, Christofk HR. Doxycycline Alters Metabolism and Proliferation of Human Cell Lines. PLoS ONE. 2013;8(5). doi:10.1371/journal.pone.0064561
47. Fonseca I, Horta C, Ribeiro AS, Sousa B, Marteil G, Bettencourt-Dias M, Paredes J. Polo-like kinase 4 (Plk4) potentiates anoikis-resistance of p53KO mammary epithelial cells by inducing a hybrid EMT phenotype. Cell Death and Disease. 2023;14(2). doi:10.1038/s41419-023-05618-1
48. Guderian G, Westendorf J, Uldschmid A, Nigg EA. Plk4 trans-autophosphorylation regulates centriole number by controlling βTrCP-mediated degradation. Journal of Cell Science. 2010;123(13):2163–2169. doi:10.1242/jcs.068502
49. Chung S, Kim SH, Seo Y, Kim SK, Lee JY. Quantitative analysis of cell proliferation by a dye dilution assay: Application to cell lines and cocultures. Cytometry Part A. 2017;91(7). doi:10.1002/cyto.a.23105
50. Lenski RE, Rose MR, Simpson SC, Tadler SC. Long-term experimental evolution in Escherichia coli. I. Adaptation and divergence during 2000 generations. American Naturalist. 1991;138(6). doi:10.1086/285289
51. Dobzhansky T. On Some Fundamental Concepts of Darwinian Biology. In: Evolutionary Biology. 1968. doi:10.1007/978-1-4684-8094-8_1
52. Melnyk AH, Wong A, Kassen R. The fitness costs of antibiotic resistance mutations. Evolutionary Applications. 2015;8(3):273–283. doi:10.1111/eva.12196
53. Fava LL, Schuler F, Sladky V, Haschka MD, Soratroi C, Eiterer L, Demetz E, Weiss G, Geley S, Nigg EA, et al. The PIDDosome activates p53 in response to supernumerary centrosomes. Genes and Development. 2017;31(1):34–45. doi:10.1101/gad.289728.116
54. Burigotto M, Mattivi A, Migliorati D, Magnani G, Valentini C, Roccuzzo M, Offterdinger M, Pizzato M, Schmidt A, Villunger A, et al. Centriolar distal appendages activate the centrosome-PIDDosome-p53 signalling axis via ANKRD26. The EMBO Journal. 2021;40(4):e104844. https://www.embopress.org/doi/abs/10.15252/embj.2020104844. doi:https://doi.org/10.15252/embj.2020104844
55. Evans LT, Anglen T, Scott P, Lukasik K, Loncarek J, Holland AJ. ANKRD26 recruits PIDD1 to centriolar distal appendages to activate the PIDDosome following centrosome amplification. The EMBO Journal. 2021;40(4). doi:10.15252/embj.2020105106
56. Ozaki T, Nakagawara A. Role of p53 in Cell Death and Human Cancers. Cancers. 2011;3(1):994–1013. https://www.mdpi.com/2072-6694/3/1/994. doi:10.3390/cancers3010994

57. Kumar A, Herbein G. Epigenetic regulation of human cytomegalovirus latency: An update. Epigenomics. 2014;6(5). doi:10.2217/epi.14.41
58. Coelho PA, Bury L, Shahbazi MN, Liakath-Ali K, Tate PH, Wormald S, Hindley CJ, Huch M, Archer J, Skarnes WC, et al. Over-expression of Plk4 induces centrosome amplification, loss of primary cilia and associated tissue hyperplasia in the mouse. Open Biology. 2015;5(12). doi:10.1098/rsob.150209
59. Arquint C, Nigg EA. The PLK4–STIL–SAS-6 module at the core of centriole duplication. Biochemical Society Transactions. 2016;44(5):1253–1263. doi:10.1042/bst20160116
60. Ohta M, Watanabe K, Ashikawa T, Nozaki Y, Yoshiba S, Kimura A, Kitagawa D. Bimodal Binding of STIL to Plk4 Controls Proper Centriole Copy Number. Cell Reports. 2018;23(11):3160–3169.e4. doi:10.1016/j.celrep.2018.05.030
61. Ohta M, Ashikawa T, Nozaki Y, Kozuka-Hata H, Goto H, Inagaki M, Oyama M, Kitagawa D. Direct interaction of Plk4 with STIL ensures formation of a single procentriole per parental centriole. Nature communications. 2014;5:5267. http://www.nature.com/ncomms/2014/141024/ncomms6267/abs/ncomms6267.html%5Cnhttp://www.ncbi.nlm.nih.gov/pubmed/25342035%5Cnhttp://www.pubmedcentral.nih.gov/articlerender.fcgi?artid=PMC4220463. doi:10.1038/ncomms6267
62. Kerschner-Morales SL, Kühne M, Becker S, Beck JF, Sonnemann J. Anticancer effects of the PLK4 inhibitors CFI-400945 and centrinone in Ewing's sarcoma cells. Journal of Cancer Research and Clinical Oncology. 2020;146(11). doi:10.1007/s00432-020-03346-z
63. Cabrera RM, Mao SPH, Surve CR, Condeelis JS, Segall JE. A novel neuregulin - jagged1 paracrine loop in breast cancer transendothelial migration. Breast Cancer Research. 2018;20(1). doi:10.1186/s13058-018-0960-8